

Regionalization-Regionalization in global hydrological models and its impact on ~~global~~ runoff simulations: A case study using the ~~global hydrological model~~ WaterGAP3 (v 1.0.0)

Jenny Kupzig¹, Nina Kupzig², Martina Flörke¹

¹Institute of Engineering Hydrology and Water Resources Management, Ruhr-University, 44801, Bochum, Germany

²Faculty of Management and Economics, Ruhr-University, 44780, Bochum, Germany

Correspondence to: Jenny Kupzig (jenny.kupzig@rub.de)

Abstract:

Valid simulation results from global hydrological models (GHMs), such as WaterGAP3, are essential to detecting hotspots or studying patterns in climate change impacts. However, the lack of worldwide monitoring data makes it challenging to adapt GHMs' parameters to enable such valid simulations globally. Therefore, ~~regionalization~~ regionalization is necessary to estimate parameters in ungauged basins. This study presents ~~the results of new regionalization-regionalization~~ methods for ~~the first time applied on the GHM~~ WaterGAP3 ~~and~~. It aims to provide insights into (1) selecting a suitable ~~regionalization-regionalization method method~~ and (2) evaluating its impact on ~~the runoff~~ simulation. ~~In this study, Our results suggest that machine learning based methods may be too flexible for regionalizing WaterGAP3 due to a significant performance loss between training and testing. four regionalization methods have been identified as appropriate for WaterGAP3. These methods span the full spectrum of methodologies, i.e., regression-based methods, physical similarity, and spatial proximity, using traditional and machine learning-based approaches. Moreover, the methods differ in the descriptors used to achieve optimal results, although all utilize climatic and physiographic descriptors. This demonstrates (1) that different methods use descriptor sets with varying efficiency and (2) that combining climatic and physiographic descriptors is optimal for regionalizing worldwide basins. In contrast, the most basic regionalization method (using the concept of spatial proximity) outperforms most of the developed regionalization methods and a pre-defined benchmark to beat in an ensemble of split sample tests. The method selection, whether spatial proximity based or regression based, has a greater impact on the regionalization than the specific details on how the method is applied. In particular, the descriptor selection plays a subsidiary role when at least a subset of selected descriptors contains relevant information. Additionally, our research has shown/indicates that regionalization-regionalization causes/leads to spatially and temporally varying uncertainty for/in ungauged regions. For example, India and Indonesia are particularly affected by higher uncertainty/regionalization highly affects southern South America, e.g., leading to high uncertainties in the flood simulation of the Rio Deseado. y. The local impact of regionalization-regionalization propagates through the water system, also affecting in ungauged areas propagates through the water system/global estimates, e.g., as evidenced by one water balance component a changed spread of/by approximately 2400-1,500 km³ yr⁻¹ across an ensemble of five regionalization methods in simulated global runoff to the ocean on a global scale, which is in the range of inter model differences. This magnitude of the impact of regionalization-discrepancy is even more pronounced when using a regionalization method deemed unsuitable for WaterGAP3, resulting in a spread of 4,208 km³ yr⁻¹. This significant increase highlights the importance of carefully choosing regionalization~~

39 ~~methods. Further research is needed to enhance the understanding of the methods' robustness on a global scale. de-~~
40 ~~pends on the variability in regionalized values and the region's sensitivity for the analysed component.~~

41 **1. Introduction**

42 Global hydrological models (GHMs) are developed and applied worldwide, e.g., to detect hotspots and examine
43 patterns of climate change impacts on the terrestrial water cycle (e.g., Barbarossa et al., 2021; Boulange et al.,
44 2021). Valid model results are a prerequisite to draw robust conclusions. For valid modelling results, it is beneficial
45 to adjust the parameter values to adapt the models to different basin processes (Gupta et al., 1998). This adaptation
46 is usually modified and evaluated (in a loop) by comparing the simulated model output, often discharge, with the
47 monitored data. However, this parameter adjustment for GHMs is challenging due to the lack of global monitoring
48 data. Consequently, parameter adjustment for GHMs can be based not only on monitored data (i.e., calibration)
49 but also on estimating parameter values for ungauged basins (i.e., ~~regionalization~~regionalization).

50 ~~Regionalization~~Regionalization defines ~~is~~ the estimation ~~of parameter values in a model of model parameters~~ for
51 ungauged basins (Oudin et al., 2008), usually based on information from gauged basins (Oudin et al., 2010). ~~Re-~~
52 ~~gionalization~~Regionalization methods generally follow the same principle: basin characteristics (e.g., physio-
53 graphic and/or climatic) are linked to hydrological characteristics and can thus be used to estimate parameter val-
54 ues. Various ~~regionalization~~regionalization methods exist, and no overall preferred method has been found (Ayzel
55 et al., 2017; Pool et al., 2021). In contrast, the optimal ~~regionalization~~regionalization method may differ, for
56 example, regarding available information (Pagliero et al., 2019) or model structures (Golian et al., 2021). There-
57 fore, different methods should be tested to find an optimal ~~regionalization~~regionalization method for a specific
58 use case (e.g., Qi et al., 2020).

59 Evaluation is needed to assess different ~~regionalization~~regionalization methods. ~~The e~~Evaluation ~~of is particularly~~
60 ~~challenging for regionalization~~regionalization methods ~~is particularly challenging because~~because they are usu-
61 ally applied when ~~there is a lack of monitoring data is missing~~monitoring data. Therefore, ~~regionalization~~region-
62 ~~alization~~alization studies often treat gauged basins as ~~"~~"ungauged~~"~~" and perform leave-one-out cross-validation (e.g.,
63 Chaney et al., 2016) or split-sample tests (e.g., Beck et al., 2016; Nijssen et al., 2000; Yoshida et al., 2022). While
64 at the mesoscale, this evaluation is already an integral part (e.g., McIntyre et al., 2005; Parajka et al., 2005; Oudin
65 et al., 2008; Yang et al., 2020), this is sometimes not the case in global or continental studies (e.g., Müller Schmied
66 et al., 2021; Widén-Nilsson et al., 2007). Another reasonable evaluation strategy is the concept of benchmark-to-
67 beat (Schaeffli & Gupta, 2007; Seibert, 2001). Applying a benchmark-to-beat supports a comprehensive evaluation
68 of whether a new approach is functional, e.g., better than a straightforward and thus transparent method or better
69 than a predecessor. To the authors' knowledge, such a benchmark-to-beat has never been used to evaluate innova-
70 tions in ~~regionalization~~regionalization at ~~the a~~a global ~~level~~scale.

71 In general, ~~regionalization~~regionalization methods can be divided into two categories based on the parameter
72 estimation strategy: (1) regression-based and (2) distance-based (He et al., 2011). Regression-based methods de-
73 rive the relationship between basin characteristics and model parameters through fitted regression models. These
74 mathematically defined relationships are further applied to estimate model parameters of ungauged basins (e.g.,
75 Kaspar, 2004; Müller Schmied et al., 2021). A significant drawback of regression-based ~~regionalization~~regional-
76 ~~ization~~ization is the difficulty of incorporating parameter interdependencies (Poissant et al., 2017), ~~as~~as ~~Re~~Regression-based

77 approaches often assume that the dependent variables, i.e., the model parameters, are not correlated (Wagener et
78 al., 2004). Distance-based approaches transfer complete parameter sets from similar or nearby donor basins to
79 ungauged basins (e.g., Beck et al., 2016; Nijssen et al., 2000; Widén-Nilsson et al., 2007). Using an ensemble of
80 donor basins, e.g., by averaging the parameter values or model outputs, can improve the performance of such
81 methods (e.g., Arsenault & Brissette, 2014). A significant disadvantage of such methods is the clustering problem
82 of ungauged basins, i.e., the unequal distribution of gauging stations worldwide (Krabbenhoft et al., 2022). Thus,
83 basins exist where distance-based approaches will use incomparable basins to transfer parameter values due to the
84 lack of close basins.

85 Recent advances have implemented machine learning-based techniques in the context of ~~regionalization~~regional-
86 ization. For example, Chaney et al. (2016) used regression trees as an alternative to least squares regression to
87 estimate parameter values in ungauged basins. Pagliero et al. (2019) explored supervised and unsupervised clus-
88 tering methods to define the similarity of basins to transfer parameter sets. To the authors' knowledge, no study
89 has compared several traditional ~~regionalization-regionalization~~ methods with machine learning-based methods
90 for a GHM on a global scale.

91 Some ~~regionalization-regionalization~~ methods do not make a clear distinction between calibration and ~~regionali-~~
92 ~~zation~~regionalization. For example, Arheimer et al. (2020) applied a basin grouping beforehand. Then, they jointly
93 calibrated the group members to define representative parameter sets. Subsequently, the representative parameter
94 sets are transferred to other basins based on grouping rules. Another approach defines so-called transfer functions
95 (Samaniego et al., 2010) and calibrates meta-parameters instead of the model parameter values (Beck et al., 2020;
96 Feigl et al., 2022). These methods, where ~~regionalization-regionalization~~ is part of the calibration process, often
97 require a change in the calibration process itself, which is challenging for GHMs (Schweppe et al., 2022), for
98 example, due to a lack of code flexibility (e.g., Cuntz et al., 2016).

99 This study proposes an improved ~~regionalization-regionalization~~ method for the state-of-the-art GHM WaterGAP3
100 (Eisner, 2016). It compares traditional ~~regionalization-regionalization~~ methods with machine learning-based meth-
101 ods and uses a “benchmark-to-beat” and an ensemble of split-sample tests to evaluate the applied methods. Fur-
102 ther, global runoff simulations are compared to analyze the impact of regionalization methods. The overall research
103 topic is evaluating and selecting the most appropriate regionalization-regionalization methods for a GHM. Specif-
104 ically, the study has two objectives. It aims

- 105 (1) to propose an improved selection for the regionalization method for WaterGAP3 and
- 106 (2) to evaluate the impact of an improved regionalization-regionalization methods against a benchmark to-
107 beat on global runoff simulations.

108 2. Data and Methods

109 2.1 The Model: WaterGAP3

110 The GHM WaterGAP3 simulates the terrestrial water cycle, including the main water storage components and a
111 simple storage-based routing algorithm. It is a fully distributed model that operates on a five arcmin grid and
112 simulates at a daily time step. A more detailed ~~model description can~~description of the model can be found in
113 Eisner (2016).

114 In WaterGAP3, most model parameter values are set a priori, e.g., using look-up tables for albedo or rooting depth.
115 Only one parameter, γ , is calibrated, which is part of the soil moisture storage in which runoff generation processes
116 are present. The model equation for γ , which originates from the HBV-96 model (Lindström et al., 1997), is given
117 in Eq. (1). Generally, higher values of γ lead to lower runoff volumes, while lower values of γ lead to higher runoff
118 volumes. ~~This~~ model parameter is calibrated per basin within the range of 0.1 and 5. The objective function ~~for~~
119 of the calibration is to minimize the deviation between the mean annual simulated and observed river
120 discharge, i.e., the calibration aims to reduce the error in discharge volume. Given the monotonic relationship
121 between the model's parameter and the optimization function, a simple search algorithm is applied: The parameter
122 space is divided into rectangles, which are subsequently subdivided into smaller rectangles depending on the di-
123 rection γ should be modified to achieve closer alignment with the optimization target. Thus, as a result of the
124 calibration results in one, each basin has a calibrated γ value (γ) between 0.1 and 5 per basin. After the calibration,
125 a correction is applied to account for high errors in the mass balance, e.g., due to inaccuracies in global meteorolo-
126 gical forcing products. This correction ~~can only be applied in~~ is only applicable on gauged basins. It is, therefore,
127 neglected in this study.

$$128 \quad R = P_t \cdot \left(\frac{S_s}{S_{s,max}} \right)^\gamma \quad (1)$$

129 where R is the daily runoff, P_t is the daily throughfall, S_s is the actual soil storage, $S_{s,max}$ is the maximal soil
130 storage (given as a global map in Appendix A), and γ is the calibration parameter.

131 Traditionally, the regionalization process in WaterGAP3 is a simple multiple linear regression (MLR) approach to
132 estimate the calibration parameter γ for ungauged basins (e.g., Döll et al., 2003; Kaspar, 2004). The drawback of
133 MLR regarding parameter interaction can be neglected: As there is only one parameter to estimate, parameter
134 interference does not exist. Instead, the approach offers the advantage of a lightweight, transparent application that
135 can be quickly revised and adapted.

136 ~~Traditionally, the regionalization process in WaterGAP3 is a simple multiple linear regression (MLR) approach to~~
137 ~~estimate the calibration parameter γ for ungauged basins (e.g., Döll et al., 2003; Kaspar, 2004). The drawback of~~
138 ~~MLR regarding parameter interaction can be neglected: As there is only one parameter to estimate, parameter~~
139 ~~interference does not exist. Instead, the approach offers the advantage of a lightweight, transparent application that~~
140 ~~can be quickly revised and adapted. We use the regionalization approach from WaterGAP2.2d as benchmark to~~
141 ~~beat as defined in Müller Schmied et al. (2021). WaterGAP2 has a model structure and calibration process that are~~
142 ~~very similar to WaterGAP3. The main difference between these models is that WaterGAP2.2d simulates at~~
143 ~~0.5° spatial resolution. Thus, we expect the regionalization approach to be feasible for WaterGAP3.~~

144 2.2 Model Data

145 WaterGAP3 requires various input data, such as soil information, topography, or information on open freshwater
146 bodies. This study uses the same input data as Kupzig et al. (2023). For meteorological forcing, we use the global
147 data set EWEMBI (Lange, 2019). This data product includes daily global forcing data with a spatial resolution of
148 0.5 degrees (latitude and longitude) that covers a period from 1979 to 2016. Specifically, WaterGAP3 uses the
149 following forcing information from the EWEMBI data set as input:

- 150 • daily mean temperature,
- 151 • daily precipitation,

- daily shortwave downward radiation, and
- daily longwave downward radiation.

The WaterGAP3 calibration requires observed monthly river discharge data. This discharge data is subsequently transformed into annual discharge sums ~~in the calibration procedure~~ and used as a benchmark in the calibration procedure. In this study, we used discharge data from 1,861 stations that were manually verified (Eisner, 2016). To get the best data available, we have updated all available station data with recent data from The Global Runoff Data Center (GRDC, [2020](#)). All stations have at least five years of complete (monthly) station data between 1979 and 2016. For each station, a contribution area, i.e., a basin, is defined with the gridded flow-direction information obtained from WaterGAP3, ~~which is~~ based on the HydroSHEDS database (Lehner et al., 2008).

The 1,861 basins are calibrated using the above-described standard calibration approach for WaterGAP3. ~~After Following~~ the standard calibration procedure, some basins still have an insufficient model performance. In this context, we define a monthly Kling-Gupta-Efficiency (KGE) below 0.4 or more than 20 % bias in monthly flow as insufficient model performance. We underscore the importance of minimizing the error in discharge volume by defining it as an additional criterion corresponding to the optimization target during calibration. ~~i.e., more than 20% bias in monthly discharge. These Basins not fulfilling the defined conditions regarding bias and KGE basins~~ are neglected in further analysis to avoid high parameter uncertainty due to errors in input data, model structure, or discharge data affecting the analysis. ~~Further~~, we have excluded all basins with less than 5000 km² (inter-) basin size ~~to from~~ the next upstream basin. We assume that this inter-basin size is large enough to assume a certain degree of interdependency between nested basins. In total, ~~1,236,933 basins~~ out of 1,861 basins are selected for regionalization-regionalization (~~323-626~~ are neglected due to insufficient low model performance, and 302 are neglected due to insufficient-inadequate basin size).

Figure 1 ~~Figure 1a~~ shows a map of the depicts the worldwide calibrated basins, highlighting gauged and ungauged regions. Whereas, covering most parts of North and South America are gauged. ~~However,~~ Africa and Oceania Australia remain largely ungauged. A cluster of gauged basins is ~~located~~ in Central Europe and in Eastern Asia. Gauged regions with low-insufficient model performance are mainly ~~found~~ in the Mississippi River basin, Southern Africa, ~~and~~ Australia, and large parts of Brazil. These regions are known to be challenging for GHMs (e.g., cf. Fig. 8b in Stacke & Hagemann, 2021).

Figure 1 ~~Figure 1b~~ shows the calibrated values for γ . It emerges that the calibrated values tend to be ~~at~~ at the upper and lower bounds of the parameter space. This ~~mis~~behaviour is already known (cf. Fig. 4b in Müller Schmied et al., 2021). A brief sensitivity analysis and discussion of the calibration parameter are included in Appendix B. The results of this analysis indicate that the clustering of the calibrated parameter value is not related to an inappropriate selection of the parameter bounds but instead to the absence or an insufficient representation of processes. Thus, the clustering of the calibrated values does not indicate an inadequate selection of the parameter bounds but ~~and~~ highlights the need-necessity to further develop-improve the model structure and the calibration strategy for WaterGAP3, e.g., by implementing multivariate calibration. However, this study focuses solely on analysing-analyzing and implementing a new regionalization-regionalization methods. It does not aim to enhance the model structure or to change the calibration approach-procedure of WaterGAP3. Future studies are needed to achieve the latter, as WaterGAP3 contains many hard-coded parameters or parameters defined by look-up tables that need to be

analyzed to identify and adjust sensitive parameters more accurately during calibration. To achieve the latter, future studies are needed to select sensitive parameters or advance the model structure to avoid structural errors that introduce high parameter uncertainty when applying multivariate calibration (Kupzig et al., 2023). Initial steps in this direction have already been taken for WaterGAP2 in the form of a multivariate and multi-objective case study in the Mississippi River basin (Döll et al., 2024).

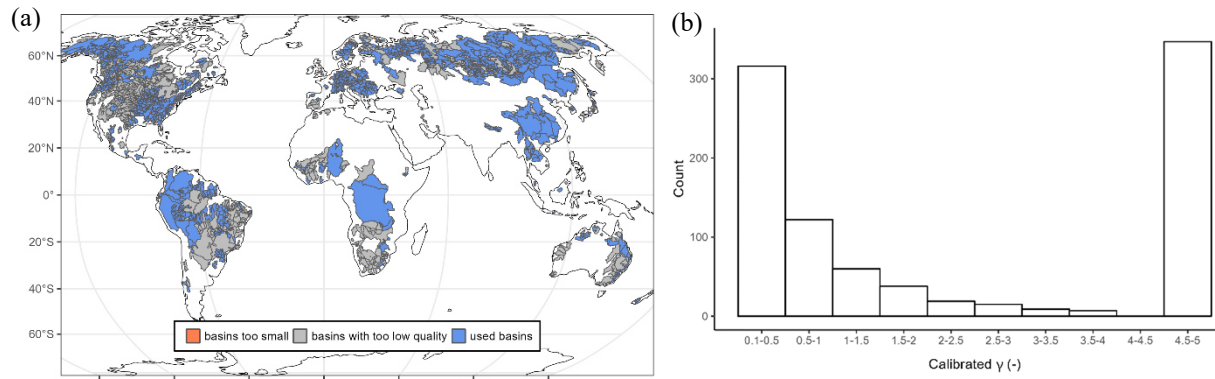


Figure 1: (a) Map of calibrated Gauged basins calibrated beforehand, highlighting basins not used for regionalization due to low insufficient model performance or too small inadequate basin size and (b) the histogram of the calibrated model parameter values of all used basins showing heavy-tails a cluster of parameter values at the parameter bounds.

2.3 Basin Descriptors

This study uses basin descriptors as predictors to drive regression-based or distance-based regionalization approaches. These basin descriptors are based on model-data used within the model simulation (as they are globally available). They are aggregated to basin values using a simple mean method to have the exact same spatial resolution as the calibrated model parameter. Thus, in the case of nested basins, the inter-basin area is used to define the basin descriptors. The selection of the predictors, i.e., basin descriptors that support the estimation of γ , is crucial for regionalization methods (Arsenault & Brissette, 2014). Typically, this selection aims to obtain the most information with the least number of predictors to (1) improve the model quality and (2) limit over-parametrization. In this study, we use 12 basin descriptors to develop regionalization methods; nine of these descriptors are physiographic, while the remaining three are climatic (see Table 1). Most descriptors are not correlated (see Appendix CA), i.e., we avoid minimize redundant information (Wagener et al., 2004).

A descriptor subset is selected based on correlation analysis between basin descriptors and calibrated γ value and entropy assessment. Pearson's correlation coefficient detects linear correlation, and Spearman's Rho and Kendall's Tau detect a non-linear correlation. Shannon entropy (Shannon, 1948) measures the information gain of the predictors explaining the calibrated γ value. The higher the information gain, the more valuable the basin descriptor is for explaining the variation in the calibrated γ value. The analysis directly evaluates the relationship between the calibrated parameter and the basin descriptors, as WaterGAP3 uses only one calibration parameter with a clear global optimum within the parameter space. An alternative would be to use flow characteristics to define the basis for regionalization (e.g., Pagliero et al., 2019). We decided to use the calibrated parameter instead of flow characteristics as it does not need any further assumption on which flow characteristics determine the model's parameter. The predictor selection is based on correlation analysis and entropy assessment. Pearson's correlation coefficient detects linear correlation, and Spearman's Rho and Kendall's Tau detect a non-linear correlation between basin

descriptors and calibrated γ values. Shannon entropy (Shannon, 1948) measures the information gain of the predictors explaining the calibrated γ value. The higher the information gain, the more valuable the basin descriptor is for explaining the variation in the calibrated γ value.

Statistical information of the evaluated basin descriptors and the corresponding correlation coefficients and the corresponding information gain are listed in Table 1. The basin descriptors demonstrate a considerable degree of variability, e.g., the basin size ranges from 5000 km² to 3,112,480 km² with a median of 13,796 km². The mean temperature varies from -19 °C to 29 °C, and the sum of precipitation ranges from 213 mm to 5,716 mm. Although there is a high degree of variability in the analyzed basin descriptors, All the basin descriptors have exhibit a low correlation coefficients with the calibrated values, e.g. For example, the permafrost coverage shows the highest strongest Pearson correlation of is -0.37 (and -0.50 for Spearman's Rho)⁶. The information gain indicates the same results as the correlation analysis, i.e., the information gain is generally relatively low, and descriptors with a higher correlation tend to have a higher information gain. The information gain shows the same result for the predictors, i.e., descriptors with a higher correlation tend to have a higher information gain. Nevertheless, the information gain is relatively low For example, the mean temperature exhibits the maximal information gain, with a maximum of 17.6 4.4% and has the second-highest correlation coefficient with a Pearson correlation of 0.34 of the information explained by the temperature descriptor.

Table 1: Basin descriptors: statistical information, correlation, and entropy assessment. Selected physiographic and climatic basin descriptors are written in bold.

	Basin Descriptor	Attribute Information				Entropy & Correlation			
		Min	Max	Mean	Median	IG (%) ¹	Pearson	Spearman	Kendall
physiographic	Soil Storage (mm)	12.405	610.469	220.805	195.778	13.07	-0.21	-0.15	-0.11
	Open Water Bodies (%)	0.000	63.960	5.521	1.812	5.65	-0.01	-0.08	-0.05
	Wetlands (%)	0.000	63.466	4.164	0.547	5.01	-0.02	-0.13	-0.09
	Size (km ²)	5000	3,112,480	37,572	13,796	1.42	-0.04	-0.04	-0.03
	Slope Class (-)	10.057	67.756	38.668	38.364	16.60	-0.31	-0.37	-0.27
	Altitude (m.a.s.l.)	30.239	4765.166	591.024	394.870	9.30	-0.18	-0.28	-0.20
	Sealed Area (%)	0.000	12.3	0.6	0.1	4.49	0.22	0.38	0.29
	Forest (%)	0.000	100.000	35.340	24.002	13.82	-0.25	-0.18	-0.14
	Permafrost & Glacier (%)	0.000	95.000	16.662	0.000	13.12	-0.37	-0.50	-0.40
climate	Mean Temperature(°C)	-18.848	28.823	7.720	7.707	17.56	0.34	0.41	0.30
	Yearly Precipitation (mm)	213.6	5,716.3	996.5	779.5	9.23	0.02	0.21	0.14
	Yearly Shortwave Downward Radiation (Wm⁻²)	1,050.6	3,043.2	1,857.9	1,759.7	15.79	0.31	0.33	0.24

¹Information gain is given in percentage of total information content in γ after Shannon (1948)

In contrast to the findings of Wagener and Wheater (2006), the correlation coefficients between the basin descriptors and the calibrated values are relatively low, indicating a weak relationship. One potential explanation for this discrepancy is that Wagener and Wheater (2006) used a smaller number of basins in southeast England, with limited versatility (e.g., regarding climate and seasonality) compared to the 933 worldwide basins used in this study. Studies using a large number of basins likely tend to find a lower correlation between catchment attributes and model parameters (Merz et al., 2004). Moreover, the clustered calibrated γ values at the bounds of the valid parameter space may disturb the results of this analysis. A possible reason for the low correlation and information gain is that the γ values are tailored within the calibration's valid parameter bounds (i.e., 0.1 and 5), resulting in heavy tails of the calibrated γ distribution. Thus, we expect the correlation to be higher, with calibrated γ reaching values higher than 5. In addition, As the calibrated value masks the effect of multiple sources of errors, such as

uncertainty in the input data, model structure, or varying hydrological processes, finding a meaningful relationship between catchment characteristics and calibrated values is challenging.

Because the basis for the descriptor selection seems uncertain, given the low correlation and the named constraints, we additionally run the regionalization methods with all descriptors to evaluate the descriptor selection. Further on, to ascertain the advantage of integrating climatic descriptors, we run the regionalization methods using either physiographic or climatic descriptors. Thus, there might be more complex relationships between the descriptors and the calibrated parameter, which are only partially captured by this analysis. Nevertheless, the results of this analysis indicate descriptors that may be more useful than others in defining a regionalization method. In total, we used implement regionalization methods using four groups of basin descriptors to implement the regionalization methods by selecting basin descriptors with the highest correlation coefficients and information gain:

- "cl":: two correlated all three climatic descriptors, (mean temperature, annual shortwave radiation),
- "p":: three correlated all nine physiographic descriptors (slope class, forest %, permafrost %),
- "p+cl": all 12 descriptors, and
- "p+subset":: two correlated climatic descriptors (mean temperature, annual shortwave radiation) & three correlated physiographic descriptors (slope class, forest %, permafrost %), and
- "all": all 12 descriptors (as a control group to examine the effect of using correlated descriptors).

Table 1: Basin descriptors used in the regionalization methods: statistical information, correlation, and entropy assessment. Selected physiographic and climatic basin descriptors are shaded in grey.

	Basin Descriptor	Attribute Information				Entropy & Correlation			
		Min	Max	Mean	Median	IG (%)	Pearson	Spearman	Kendall
physiographic	Soil Storage (mm)	8.994	677.950	219.071	192.006	10.19	-0.20	-0.16	-0.12
	Open Water Bodies (%)	0.000	77.125	7.979	2.376	5.22	0.01	-0.05	-0.03
	Wetlands (%)	0.000	73.181	6.134	0.721	4.60	0.02	-0.07	-0.05
	Size (km ²)	5000	3112480	36811	13850	1.08	-0.03	-0.01	-0.01
	Slope Class (-)	10.057	67.756	37.739	36.986	14.22	-0.27	-0.31	-0.23
	Altitude (m.a.s.l.)	22.324	4765.166	630.826	412.414	7.29	-0.11	-0.19	-0.14
	Sealed Area (%)	0.000	12.3	0.5	0	3.25	0.18	0.34	0.25
	Forest (%)	0.000	100.000	32.037	18.245	11.50	-0.27	-0.21	-0.16
	Permafrost & Glacier (%)	0.000	95.000	15.316	0.000	10.96	-0.36	-0.47	-0.37
climate	Mean Temperature (°C)	-18.848	28.998	-7.769	6.562	14.36	0.34	0.39	0.29
	Yearly Precipitation (mm)	73.1	5716.3	950.6	743.5	7.95	0.01	0.18	0.13
	Yearly Shortwave Downward Radiation (Wm ⁻²)	1050.6	33098.4	1887.5	1777.2	13.05	0.33	0.34	0.25

2.4 Regionalization Methods

In our study, we test several traditional and machine learning-based regionalization methods against each other and a defined benchmark-to-beat to find the most suitable regionalization methods for WaterGAP3. At the global scale, regionalization is particularly challenging due to (1) the lack of high-quality data, (2) the diversity of dominant hydrological processes in basins, and (3) the high computational demands of the models. Therefore, a robust regionalization method that applies to a wide variety of basins and is not computationally demanding should be selected for a global application. Therefore, a regionalization method that is robust, applicable to a wide variety of basins, and not computationally demanding should be chosen.

279 We test three common traditional approaches and two machine learning-based approaches using the concepts of
280 spatial proximity, physical similarity, and regression-based methods. As WaterGAP3's model calibration is very
281 rigid and has only one parameter, it is not feasible to implement and test regionalization methods that incorporate
282 regionalization into the calibration process, such as transfer functions. In addition, we avoid high computational
283 demands as all evaluated methods are applicable after the calibration, i.e., without running the model.~~We test three~~
284 ~~common traditional approaches: spatial proximity, physical similarity, and regression-based methods, as well as~~
285 ~~two machine learning-based approaches. These machine learning-based approaches are alternatives to traditional~~
286 ~~physical similarity and regression-based methods. As the model calibration of WaterGAP3 is very rigid and has~~
287 ~~only one parameter, it is not feasible to implement and test regionalization methods that incorporate regionalization~~
288 ~~into the calibration process, such as transfer functions. In addition, we avoid high computational demands as all~~
289 ~~methods can be applied after the calibration, i.e., without running the model.~~

290 As the calibration of WaterGAP3 results in a parameter distribution with a cluster of parameter values at the
291 parameter bounds, we implement a so-called "tuning" to introduce information about the parameter space into
292 regionalization. In detail, we apply a simple threshold-based approach to shift the regionalized parameter values
293 to the extremes, i.e., $\gamma_{est} < \gamma_1 \rightarrow \gamma_{reg} = 0.1$ and $\gamma_{est} > \gamma_2 \rightarrow \gamma_{reg} = 5.0$. The thresholds γ_1 and γ_2 are defined
294 by applying the k-means algorithm with three centers to the calibrated parameter values. This clustering results in
295 three clusters: one for low, one for medium, and one for high γ values. Subsequently, γ_1 refers to the highest γ
296 value of the low cluster and γ_2 refers to the lowest γ value of a high cluster.

297 ~~To~~~~To evaluate~~~~evaluate~~ the ~~regionalization~~~~regionalization~~ methods, we implement an ensemble of split-sample
298 tests. Specifically, we randomly split the basins into 50% gauged (for training) and 50% pseudo-ungauged (for
299 testing) basins. ~~This~~ is split has a relatively high percentage of pseudo-ungauged basins, accounting for many miss-
300 ing gauges worldwide. We fit the methods and apply them to the training and testing data sets. The split-sample
301 test is repeated 100 times ~~with~~~~by~~ randomly ~~selected~~~~splitting the basins~~ basins for training and testing to account
302 for sampling effects.

303 As there is only one calibration parameter, γ , this parameter has a global optimum per basin. Consequently, the
304 quality of training and testing is directly assessed by the deviation between the ~~predicted~~~~regionalized~~ and the
305 calibrated value for γ . The closer the regionalized values are to the calibrated ones, the more accurate the predic-
306 tion. We assess the prediction accuracy by the logarithmic version of the mean absolute error (logMAE) to account
307 for the decreasing sensitivity of γ for higher values (see Appendix B). Thus, the mean absolute error (MAE), an
308 easy to interpret measure, is used to evaluate the prediction accuracy.~~The lower the logMAE, the better the pre-~~
309 ~~diction; an MAE zero value of zero in logMAE expresses no error. In our case, an MAE of 2.1 corresponds to the~~
310 ~~error when using the mean calibrated γ value as the predicted value.~~~~The regionalization~~~~regionalization~~ method is
311 robust if the prediction accuracy is similar in training and testing. A generally good performance, i.e., small log-
312 MAE values, indicates that the regionalization~~regionalization~~ method suits WaterGAP3. The comparison of γ
313 values enables applying a wide range of regionalization methods and sets of descriptors, as no computationally
314 intensive model simulation is required. However, it assumes that deviations in γ lead, in turn, to deviations in
315 discharge, which is only partially true because of varying parameter sensitivity in basins (e.g., Kupzig et al., 2023).
316 To validate that the logMAE is a sufficient approximator for the regionalization performance in WaterGAP3, we
317 use one representative split-sample from the ensemble to compare the accuracies in simulated discharge for dif-
318 ferent regionalization methods.

319 **Regression-based methods**

320 ~~The traditionally used regionalization approach of WaterGAP3 is a regression-based MLR. As the benchmark-to-~~
321 ~~beat, we use the regionalization approach from WaterGAP2.2d defined in Müller Schmied et al. (2021). We con-~~
322 ~~sider it a suitable benchmark-to-beat given that WaterGAP2 has a model structure and calibration process that is~~
323 ~~very similar to WaterGAP3. The main difference between these models is that WaterGAP2 simulates at 0.5°spatial~~
324 ~~resolution. The benchmark-to-beat consists of "a multiple linear regression approach that relates the natural loga-~~
325 ~~rithm of γ to basin descriptors (mean annual temperature, mean available soil water capacity, fraction of local and~~
326 ~~global lakes and wetlands, mean basin land surface slope, fraction of permanent snow and ice, aquifer-related~~
327 ~~groundwater recharge factor)". (Müller Schmied et al., 2021) We fit this regression model to our data and define~~
328 ~~the quality of this approach as the benchmark-to-beat. Moreover, we test an independent MLR approach without~~
329 ~~using the logarithmical scaling of γ and using the above-defined sets of basin descriptors. For MLR and the bench-~~
330 ~~mark-to-beat, we use the lm() function of the R package stats (R Core Team, 2020). After applying the regression~~
331 ~~model, we adjust the estimated parameter values to ensure that the estimated values range between 0.1 and 5.~~

332 ~~For the traditional regression-based methods, we use the lm() function of the R package stats (R Core Team, 2020)~~
333 ~~to implement an MLR. After applying the regression model, we adjust the estimated parameter values to ensure~~
334 ~~that the estimated values range between 0.1 and 5. As the calibration of WaterGAP3 results in a parameter distri-~~
335 ~~bution with heavy tails, we implement a so-called "tuning approach" to introduce this information into regionali-~~
336 ~~zation. In detail, we apply a simple threshold-based approach to adjust the regionalized parameter values to the~~
337 ~~extremes, i.e., $\gamma_{est} < \gamma_{\pm} \rightarrow \gamma_{reg} = 0.1$ and $\gamma_{est} > \gamma_{\pm} \rightarrow \gamma_{reg} = 5.0$. A simple clustering, i.e., the k means algo-~~
338 ~~rithm with three centres, defines these thresholds.~~

339 Furthermore, a machine learning-based method, ~~namely~~ random forest (RF), is tested for ~~regionalization~~
340 ~~regionalization as an alternative to MLR~~. Here, we implement the random forest algorithm with the randomForest() func-
341 tion from the R package randomForest (Liam & Wiener, 2002), which is based on Breimann (2001). The algorithm
342 uses an ensemble of decision trees, making the decision human-like. It is relatively robust because it incorporates
343 random effects into the training process. To implement this randomness, we define ~~that the algorithm~~
344 ~~as one that~~ can choose between two randomly selected predictors at each node. ~~We use an,~~ using an ensemble of
345 200 trees, ~~the same combinations of predictors and the same tuning as for MLR.~~

346 ~~The benchmark to beat defined in Müller Schmied et al. (2021) also uses an MLR approach. This MLR approach~~
347 ~~relates the natural logarithm of γ to the following basin descriptors: mean temperature, mean available soil water~~
348 ~~capacity, fraction of open freshwater bodies, mean slope, mean fraction of permafrost coverage and an aquifer-~~
349 ~~related groundwater recharge factor. Thus, the main differences between the benchmark to beat and our defined~~
350 ~~MLR-based approach are the natural logarithm, our proposed tuning procedure for the method itself, and using the~~
351 ~~aquifer related groundwater recharge factor as a basin descriptor.~~

352 **Physical Similarity**

353 ~~For As a the~~ traditional physical similarity approach, we use Similarity Indices (in the following named with SI),
354 ~~applying. We use~~ the methodology proposed by Beck et al. (2016). The SI (see Eq. (2)) are derived using the
355 ~~defined~~ basin descriptors ~~sets mentioned above~~, and the parameter of the most similar basin is transferred to the
356 pseudo-ungauged basin. Additionally, we use an ensemble of basins to control whether an ensemble-based ap-
357 proach leads to more robust results. The optimal number of donor basins may vary between research regions and

358 hydrological models (Guo et al., 2020). Here, we use ten donor catchments (noted with "~~ensemble10~~") which
359 ~~is~~-based on Beck et al. (2016) and McIntyre et al. (2005~~6~~). Further, we apply a simple mean method for the en-
360 semble-based prediction to aggregate the ensemble of γ values into one predicted parameter value.

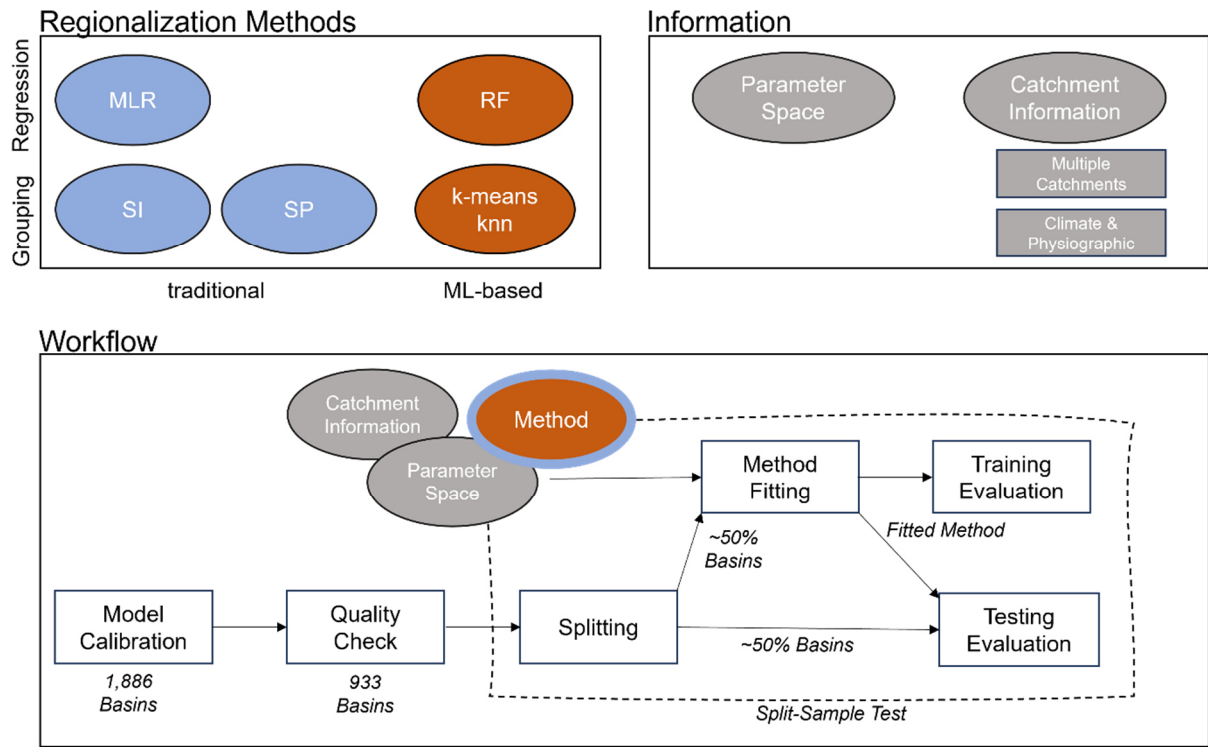
$$S_{i,j} = \sum_{p=1}^n \frac{|Z_{p,i} - Z_{p,j}|}{IQR_p} \quad (2)$$

where $S_{i,j}$ is the Similarity Index between basin i and basin j , $Z_{p,j}$ is the basin descriptor p for basin j , IQR_p is the interquartile range for basin descriptor p among all (gauged) basins, and n is the number of all basin descriptors used.

As an alternative a-machine learning-based approach, we apply a simple k-means algorithm. We selected the k-means algorithm because it is one of the most widely used clustering algorithms (Tongal & Sivakumar, 2017). It is easy to understand and use. The algorithm `kmeans()` is implemented in the R base package `stats`. It aims to ~~maximize~~ maximize variation between groups and ~~minimize~~ minimize variation within groups. The number of clusters to use is determined by multiple indices calculated with the R package `NbClust` (Charrad et al., 2014). For all 933 basins and the defined sets of basin descriptors, most indices defined three as the optimal number of clusters. Accordingly, wWe use three clusters to generate the groups of basins. As different scales of the predictor values can affect the clustering, a rescaling with min-max-~~normalization~~ normalization (see Eq. (3)) is performed on the training set and applied to the testing set. After the grouping, the mean γ value is assigned as a representative calibrated value to the corresponding basin group. To estimate the corresponding group for a pseudo-ungauged basin, the `knn` algorithm is used, and the representative γ value of the group is assigned to the pseudo-ungauged basin. This algorithm is implemented by the `knn()` function of the R package class (Venables & Ripley, 2002). Since ~~this method~~ the k-means method is less flexible than SI, we implement a highly flexible version, using the `knn` algorithm directly to define the donor basin most similar to each ungauged basin. ~~of k-means with 162 groups, where each ungauged basin is sorted into a very small basin group.~~ Using this highly flexible version the `knn` algorithm directly of k-means, we test ~~whether the potential differences between SI and k-means are based on the degree of flexibility~~ how beneficial it is to create groups of similar basins using the `kmeans` algorithm and regionalize the parameter with a representative mean value.

$$Z'_{p,j} = \frac{Z_{p,j} - \min_{j \rightarrow m}(Z_{p,j})}{\max_{j \rightarrow m}(Z_{p,j}) - \min_{j \rightarrow m}(Z_{p,j})} \quad (3)$$

where $Z'_{p,j}$ is the ~~normalise~~ normalized basin descriptor p for basin j , $Z_{p,j}$ is the basin descriptor p for the basin j , m is the number of (gauged) basins.

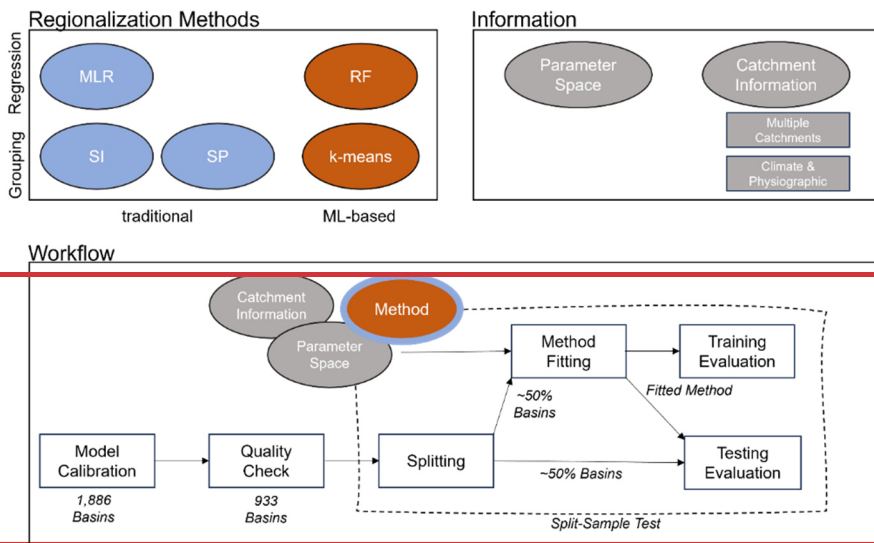


386

387 **Figure 2: Experimental setup of the study: regionalization methods, used modifications and information, and the general workflow (MLR: Multiple Linear Regression, SI: Similarity Indices, SP: Spatial Proximity, RF: RandomForest).**

388

389



390

391 **Figure 2: Experimental setup of the study: regionalization methods, used modifications and information and the general workflow (MLR: Multiple Linear Regression, SI: Similarity Indices, SP: Spatial Proximity, RF: RandomForest).**

392

393 Spatial Proximity

394 The spatial proximity approach is one of the easiest to regionalize regionalize parameter values. However, it is
 395 also often criticized-criticized that nearby basins do not necessarily have the same hydrological behavior
 396 (Wagener et al., 2004). Furthermore, its performance depends on the density of the network of gauged basins
 397 (Lebecherel et al., 2016). The dependency on network density is particularly challenging for global applications
 398 where large parts of the world are ungauged (e.g., northern Africa). Nevertheless, the approach has been success-
 399 fully applied in other studies (e.g., Oudin et al., 2008; Qi et al., 2020), even globally (Widén-Nilsson et al., 2007).

400 Here, we take the distance between the centroids of the basins as the reference for the spatial distance between
401 basins, as done by others (Oudin et al., 2008). We use the abbreviation SP in the text below to refer to the spatial
402 proximity approach. Figure 2 ~~Figure 2~~ provides an overview of the applied ~~regionalization~~ regionalization methods
403 and information used for the experimental setup.

404 3. Results and Discussion

405 3. Results and Discussion

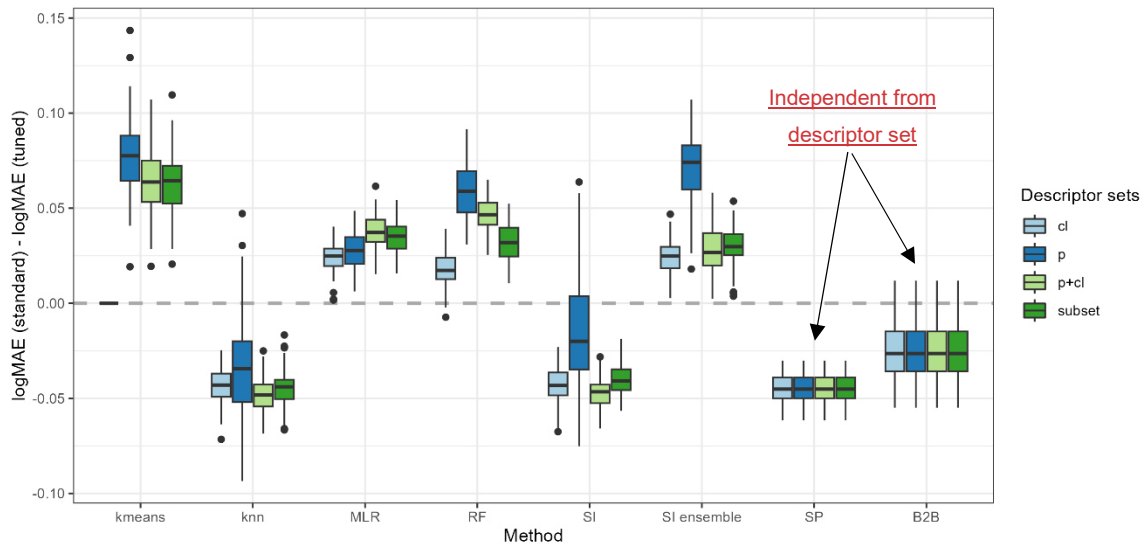
406 3.1 Evaluating ~~the effect of Traditional Methods~~ tuning

407 First, the impact of the tuning approach on the regionalization approaches is evaluated. Therefore, Fig. 3 depicts
408 the differences in logMAE between the standard and tuned approaches in testing, i.e., using the pseudo-ungauged
409 basins. A positive difference in logMAE indicates an increase in accuracy, whereas a negative difference indicates
410 a decrease in accuracy due to the tuning.

411 Using the tuning thresholds of about 1.1 and 3.4 for γ_1 and γ_2 , respectively, enhances the predictive accuracy for
412 kmeans, MLR, RF, and the ensemble approach of SI. The most remarkable improvement for kmeans, RF, and SI
413 ensemble is achieved when all physiographic descriptors are used as input (mean improvement of 0.077, 0.058,
414 and 0.071, respectively). MLR shows the most significant improvement when using all available descriptors (mean
415 improvement of 0.038). In contrast, the tuning decreases the performance for knn, SI, and SP, with a mean degra-
416 duction between -0.02 and -0.05. Unlike the enhanced regionalization techniques, these methods transfer single-
417 basin information to ungauged regions. Thus, the tuning disturbs the use of single-basin information yet simulta-
418 neously enhances the performance of methods that transfer multi-basin information. The disturbance or improve-
419 ment is probably related to the capability of the methods representing the clustering of parameter values at the
420 extremes: Whereas the multi-basin information transfer implies a smoothing and thus suffers from a lack of rep-
421 resenting the extremes, the single-basin information transfer exhibits no such a smoothing.

422 The exception from the above-defined rule is the benchmark-to-beat approach. The benchmark-to-beat is the only
423 approach that uses logarithmic scaled γ values when fitting the model. This logarithmic transformation leads to an
424 increase in estimating small values. Thus, when the benchmark-to-beat is tuned, more basins with higher calibrated
425 γ values receive low estimates. The tuning intensifies this effect, leading to a decrease in the accuracy of the
426 logMAE from the standard to the tuned version. Thus, for models using logarithmical transformed γ values, the
427 defined thresholds for the tuning are not appropriate.

428 Applying knowledge of the optimal parameter space enhances the quality of regionalization for methods transfer-
429 ring multi-basin information in case the tuning thresholds are appropriate. This positive effect is not surprising, as
430 incorporating a priori information about parameter distribution strengthens parameter estimation (e.g., described
431 in Tang et al. (2016) using the Bayes Theorem). However, for single-basin transfer, which already represents the
432 parameter space well, i.e., the clustering of γ at the extremes, the tuning disturbs the performance. This indicates
433 that such tuning needs to be cautiously introduced as there is the risk of decreasing the accuracy of regionalization.



434

435 **Figure 3: Changes in performance between standard and tuned versions for all applied regionalization approaches.**
 436 **Positive values indicate an improvement related to the tuning.**

437 **3.2 Evaluating descriptor subsets & algorithm selection**

438 Different descriptor sets yield different performances in regionalizing γ . Table 2 shows the median of all logMAE
 439 values for the testing. For a complete overview of the results of the split-sample test ensemble, see Appendix D.
 440 Evaluating Table 2 reveals that the selected subset or all descriptors consistently yield the best performance across
 441 all regionalization methods. In both variants of the ensemble approach of SI, the tuned version of the no-ensemble
 442 approach of SI, and the standard version of RF, the selected subset yields the best results. For all other methods,
 443 using all descriptors yields the best results. Hence, all methods perform best when combining climatic and physi-
 444 ographic descriptors. This benefit of using climatic and physiographic descriptors is consistent with others that
 445 often apply a combination of climatic and physiographic descriptors, achieving optimal regionalization results
 446 (e.g., Oudin et al., 2008; Reichl et al., 2009).

447 The machine learning-based approaches seem to benefit most when using more information displaying an im-
 448 provement for all methods (knn, kmeans, and RF) and both variants (standard and tuned) ranging from "cl", "p",
 449 "subset" to "p+cl". This is not surprising as machine learning is developed to deal with big data sets. The traditional
 450 methods MLR and SI do not exhibit such a distinct pattern. The (weakly) correlated subset of climatic and physi-
 451 ographic descriptors yields the best results for SI. As utilizing all descriptors decreases the performance slightly,
 452 the results indicate that uncorrelated descriptors may disturb the performance of this approach. For MLR, the
 453 meaning of physiographic information is highest, resulting in the best ("p+cl") and second best ("p") results. The
 454 disparate performance of the regionalization methods when using different descriptor sets indicates that different
 455 methods use descriptor sets with varying efficiency. It also emphasizes that the selection of descriptors impacts
 456 the regionalization method's results, as noted by others (Arsenault & Brissette, 2014). Consequently, the above-
 457 performed analysis defining a descriptor subset lacks universal validity as methods exist where the defined subset
 458 is outperformed. Instead, the validity of this approach is most closely aligned with the SI approaches.

459 Although the algorithms kmeans and knn are similar, they yield considerably different performances in Table 2.
 460 As knn shows a logMAE of 0.432 at best, the kmeans algorithm performs poorly, resulting in the best logMAE of
 461 0.472. This indicates that applying the kmeans clustering algorithm to transfer averaged parameters is inappropri-
 462 ate for WaterGAP3. This may be attributed to the reduced flexibility of the approach, which entails estimating

only three γ values due to the optimal, though limited, number of centers. The ensemble SI approach consistently outperforms the no-ensemble SI approach in almost all variants. The positive effect of an ensemble approach for SI has already been noted (Oudin et al., 2008). Therefore, it is recommended that the number of donor basins derived from the literature be adopted in future applications to be optimal for WaterGAP3, likely resulting in higher performance.

Only a few regionalization methods outperform the benchmark-to-beat. The best descriptor sets of tuned MLR, RF, and SI ensemble approach have a logMAE of 0.427, 0.403, and 0.409, respectively. The standard version of knn ("p+cl") and SP yield 0.432 and 0.454 in logMAE, respectively. Additionally, two variants of the standard SI approaches outperform the benchmark-to-beat yet exhibit inferior results compared to the selected tuned approach. All other regionalization methods show higher logMAE values than the benchmark-to-beat. These methods are considered insufficient in terms of performance to regionalize γ in WaterGAP3. As the benchmark-to-beat outperforms all kmeans approach variants, it is deemed unsuitable for regionalizing γ for WaterGAP3 and, therefore, excluded from further analysis.

Table 2: Median logMAE of 100 split-samples for pseudo-ungauged basins, i.e., in testing, for all regionalization methods applying four sets of descriptors for a) the standard version and b) the tuned version. The bold numbers indicate a better performance than the benchmark-to-beat. Thicker edges mark best-performing variants, which are chosen for further analysis. Grey-shaded cells indicate worst-performing variants, which were taken to validate the assumption that lower logMAE values result in lower KGE values.

(a)

test (median)	MLR	RF	SI		kmeans	knn	SP	B2B
			no ens.	ensemble				
cl	0.552	0.483	0.496	0.483	0.619	0.501	0.454	0.461
p	0.479	0.465	0.487	0.480	0.551	0.477		
p+cl	0.464	0.464	0.454	0.462	0.534	0.432		
subset	0.488	0.488	0.461	0.439	0.539	0.467		

(b)

test* (median)	MLR	RF	SI		kmeans	knn	SP	B2B
			no ens.	ensemble				
cl	0.529	0.467	0.537	0.459	0.619	0.546	0.502	0.488
p	0.441	0.416	0.532	0.455	0.515	0.521		
p+cl	0.427	0.403	0.503	0.435	0.472	0.480		
subset	0.453	0.408	0.501	0.409	0.477	0.509		

The well-performing SP on a global scale is surprising as the distances between basins are potentially long, and hydrological processes may strongly vary. It is probably beneficial for the SP approach that γ comprises all kinds of errors, e.g., spatially localized errors in global forcing products (e.g., Beck et al., 2017 reported errors for arid regions in the precipitation product) or inaccurately represented processes for larger regions. Thus, the estimation of γ might be appropriate, but not because of the same hydrological behavior but due to the same kind of errors.

The RF approach is outstanding, as it shows a massive loss in performance from training to testing (see Appendix D). In detail, the logMAE in testing is about twice the logMAE in training. In comparison, other methods show results from 95.6 % to 101.4 %. This performance loss indicates that RF is not a robust regionalization method for WaterGAP3. Other studies that reported the good performance of RF for regionalization have not investigated the

490 stability of the performance from training to testing (Golian et al., 2021; Wu et al., 2023). Likely, the mathematical
491 problem of predicting the calibrated parameter for WaterGAP3, with all its challenges (e.g., tailored parameter
492 space, clustered calibrated parameter, and incorporation of many sources of errors), cannot be adequately solved
493 by RF. Thus, although RF is known to be especially robust among other machine learning-based techniques, it
494 shows symptoms of over-parameterization. This indicates that the algorithm is too flexible and adjusts to noise in
495 the data, missing the underlying systematic. This lack of robustness is particularly disadvantageous since, for Wa-
496 terGAP3, regionalization is applied globally, requiring regionalizing large parts of the world. In consequence, the
497 RF approach is left out from further analysis and defined as not suitable to regionalize γ for WaterGAP3.

498 **3.3 Performance of selected algorithm in pseudo-ungauged basins**

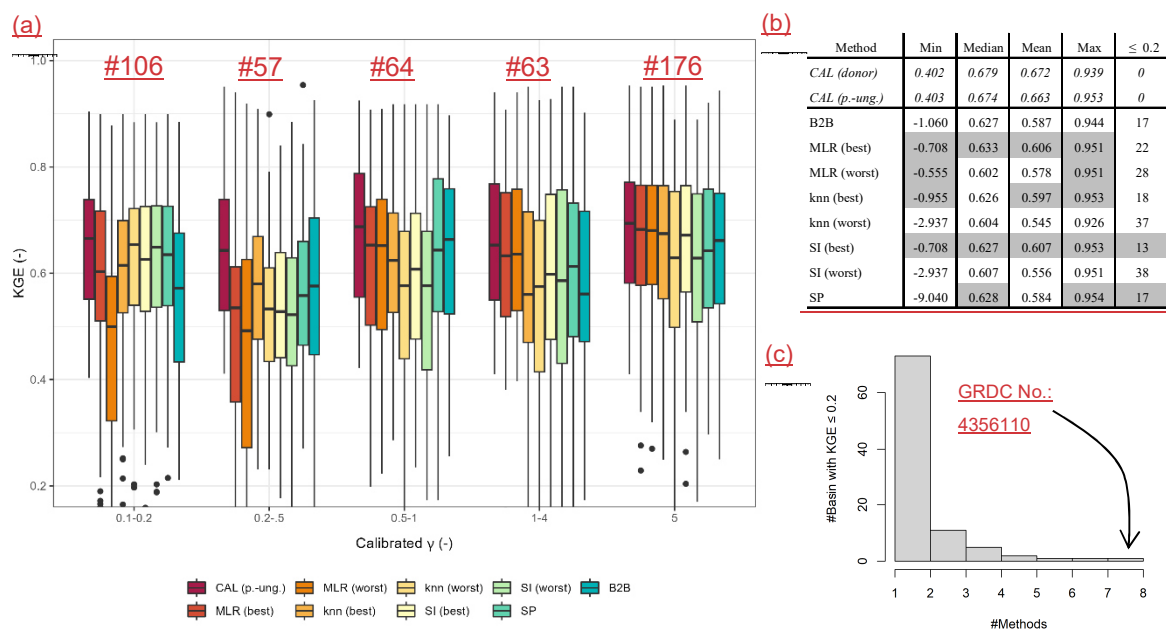
499 To avoid the high risk of sampling effect when applying the split-sample test, we conduct an ensemble of 100
500 split-sample tests analyzing the median of logMAE between regionalized and calibrated values as an indicator for
501 performance. Directly using the differences in regionalized and calibrated values is only meaningful when the
502 calibrated value represents the global optimum. As this is often not the case, e.g., due to equifinality, the perfor-
503 mance of regionalization methods is usually assessed by the accuracy of simulated discharge (e.g., Samaniego et
504 al., 2010; Arsenault & Brissette, 2014). Because WaterGAP3 requires computationally intensive simulations, run-
505 ning WaterGAP3 for all 100 split-sample tests for the selected methods is not feasible. Therefore, we select a
506 single representative split-sample to assess the quality of representing the discharge in the pseudo-ungauged basins
507 using regionalized γ values. The representative split-sample leads to comparable logMAE values to the corre-
508 sponding median of the ensemble for all regionalization methods. For the evaluation, WaterGAP3 was run for the
509 same period used in calibration (from 1979 to 2016), with the first year simulated ten times to allow for model
510 warm-up. Using this period ensures the availability of sufficient data for the evaluation (see Chapter 2.2). Further-
511 more, the differences between the monthly simulated and observed discharge are assessed using the KGE.

512 To evaluate the KGE, we select the best-performing methods that outperform the benchmark-to-beat: tuned MLR
513 "p+cl", knn "p+cl", tuned SI ensemble "subset", and SP (see Table 2). For the sake of simplicity, we further mark
514 them with "(best)". Additionally, we select three poorly performing variants to validate the assumption that meth-
515 ods resulting in higher logMAE values tend to result in lower KGE values, i.e., lower accuracy of simulated dis-
516 charge. These methods are tuned SI "cl" (logMAE: 0.537), tuned knn "cl" (logMAE: 0.546), and MLR "cl" (log-
517 MAE: 0.552). Further, we denote these methods with "worst". Applying the selected methods and the benchmark-
518 to-beat method results in eight estimates of γ for the pseudo-ungauged basins, whose performance is further eval-
519 uated in terms of simulated discharge accuracy.

520 Figure 4a shows the resulting KGE values for the evaluated regionalization methods and the calibrated version as
521 grouped boxplots for different ranges of calibrated γ . The methods show different performances for different γ
522 ranges, indicating their strengths and weaknesses. For the smallest γ range, "0.1-0.2", the selected methods that
523 perform well during the split-sample test outperform the benchmark-to-beat. The better result for minimal γ ranges
524 is probably partially related to the advantage of the tuning, which leads to more predictions of 0.1 within the
525 regionalization. The benchmark-to-beat shows the best performance for γ values between 0.2 and 0.5. The good
526 performance for basins with calibrated γ values between 0.2 and 0.5 is probably related to the benefit of using the
527 logarithmical version of γ in the benchmark-to-beat, leading to more estimates of smaller values. However, this
528 affects only 12 % of the basins, as calibrated values between 0.2 and 0.5 are not frequently present in the calibration

529 result. Generally, the differences in KGE appear higher for smaller γ values, probably due to the decreasing pa-
 530 rameter sensitivity with higher values (see Appendix B).

531 Given the variability in the performance of the regionalization methods across the depicted γ ranges, it is challeng-
 532 ing to identify an overall best regionalization method using Fig. 4a. Therefore, we compare the various metrics of
 533 the KGE values depicted in Fig. 4b. The analyzed metrics are the minimum, maximum, mean, and median. Further,
 534 we count the number of poorly performing basins, defined as basins with a KGE below 0.2. In Fig. 4b, metrics
 535 that exceed the benchmark-to-beat are grey-shaded.



536 **Figure 4: a) KGE values of pseudo-ungauged basins from split-sample test grouped by the range of calibrated γ values,**
 537 **b) selected metrics of KGE values from the pseudo-ungauged basins (better or equal performance to the benchmark-**
 538 **to-beat is highlighted in grey), and c) histogram of the number of pseudo-ungauged basins with a KGE below 0.2 and**
 539 **the corresponding number of methods exhibiting this performance loss.**

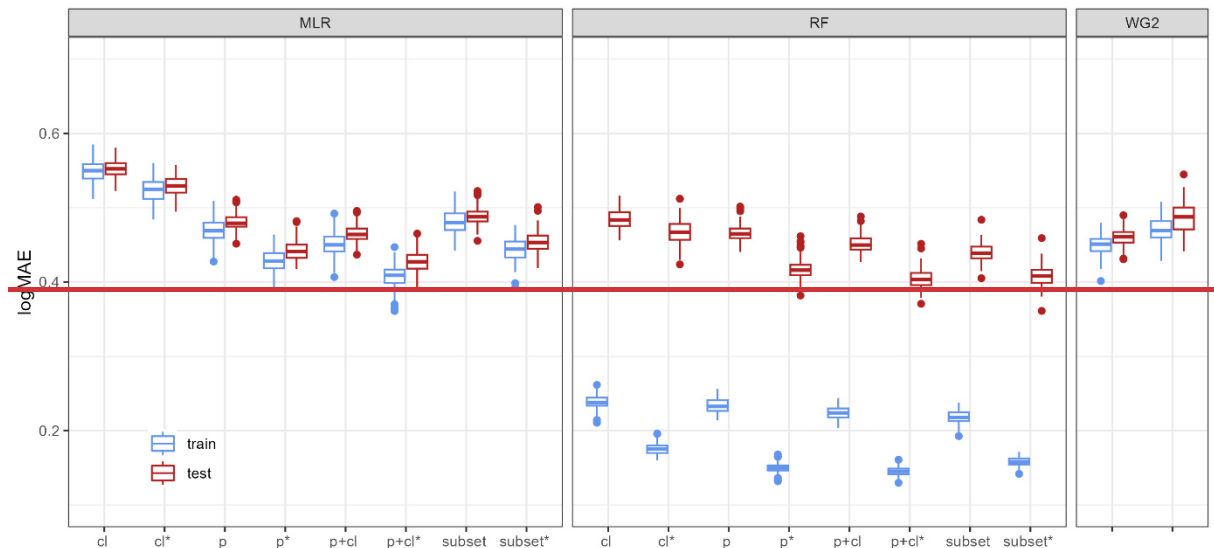
540 Comparing the KGE metrics in Fig. 4b reveals that the methods showing higher logMAE values in our split-
 541 sampling test ensemble also show lower performance in simulating discharge. For example, all mean (and median)
 542 KGE values of the "worst" methods are below the mean KGE of 0.587 from the benchmark-to-beat, ranging from
 543 0.545 to 0.578. This indicates that the used logMAE between regionalized and calibrated values is a valid tool for
 544 a preliminary selection of adequate methods for the regionalization of WaterGAP3. However, for a more compre-
 545 hensive analysis, we recommend additionally analyzing the accuracy of simulated discharges, as the logMAE of
 546 calibrated and regionalized parameter values simplifies the inherent complexity between model parameters and
 547 model performance.

548 Moreover, SI (best) outperforms the benchmark-to-beat in all listed metrics, reducing poorly performing basins
 549 and enhancing well-performing basins. MLR (best) performs very similarly to SI (best), yet it shows a higher
 550 number of basins with KGE values below 0.2. In comparison to the benchmark-to-beat, it outperforms four out of
 551 five criteria. The remaining well-performing methods, SP and knn (best), demonstrate superior or equal perfor-
 552 mance to the benchmark-to-beat in three out of five criteria. SP results in an equal number of poorly performing
 553 basins, and the minimal KGE value is lower than for the benchmark-to-beat. The knn (best) approach has a slightly
 554 worse median of KGE, i.e., -0.001, and one additional basin shows a KGE below 0.2.

555 As SI (best) outperforms the benchmark-to-beat in all metrics, we conduct a statistical test to ascertain whether
556 there is a statistically significant difference in KGE results between the methods. To this end, we use a paired
557 Wilcoxon rank sum test to test the null hypothesis of whether the KGE differs significantly in central tendency. A
558 significance level of 0.05 and an adjusted p-value are applied to correct for multiple comparisons (using the cor-
559 rection after Benjamini & Hochberg (1995)). The results demonstrate that SI (best) outperforms all "worst" meth-
560 ods and the benchmark-to-beat. However, the null hypothesis for SP and the "best" options of knn and MLR cannot
561 be rejected. Consequently, rather than identifying a single alternative to the benchmark-to-beat, we have identified
562 four.

563 Notably, all regionalization methods lead to poorly performing basins, as evidenced by the range of basins with a
564 KGE below 0.2, varying from 13 to 37. In Fig. 4c, we examine whether there are basins that all methods cannot
565 regionalize, thereby indicating a general insufficiency of the regionalization methods for these basins. The histo-
566 gram indicates that most poorly performing basins belong to a single regionalization method. The high number of
567 basins, which cannot be estimated well by a single regionalization method, illustrates the diverse shortcomings of
568 the methods. A single basin shows poor performance across all methods. This is a basin of the river El Platanito
569 in Mexico. The calibrated γ value is about 1.5, and the corresponding KGE value in calibration is 0.466. This basin
570 appears to be highly sensitive to γ , with an inaccuracy in the estimated γ having a significant impact on the accuracy
571 of river discharge. For example, the benchmark-to-beat estimates γ to 1.0, which is close to the calibrated value of
572 1.5. However, the KGE value of the simulated discharge using the benchmark-to-beat is -0.158 due to a high
573 overestimation of the variation and mean of the discharge. This high sensitivity seems outstanding and is likely
574 attributable to the absence of waterbodies and snow, supporting a potentially high impact of γ on the model simu-
575 lation (Kupzig et al., 2023) in conjunction with a relatively small basin size (ca. 6,600 km²).

576 ~~Here, we examine the traditional methods (MLR, SI, SP) by comparing the ensemble of MAEs from training and~~
577 ~~testing to each other and the benchmark to beat (see Fig. 3). Thus, applying knowledge of the optimal parameter~~
578 ~~space enhances the quality of regionalization. This positive effect is not surprising, as incorporating a priori infor-~~
579 ~~mation about parameter distribution strengthens parameter estimation (e.g., described in Tang et al., 2016 using~~
580 ~~the Bayes Theorem). As for all traditional methods, there is no significant performance loss between training and~~
581 ~~testing, we will further focus on the performance in testing for evaluating the methods. When assessing the MLR~~
582 ~~and the SI approach, it becomes apparent that using only the climatic descriptors is insufficient for regionalization~~
583 ~~as it provides worse estimates than the benchmark to beat. The exclusive selection of physiographic descriptors~~
584 ~~(slope class, forest %, and permafrost %) performs better, and yields results comparable to our benchmark to beat~~
585 ~~for both methods. Using climatic and physiographic descriptors jointly increases the performance of SI by approx-~~
586 ~~imately 0.1 in median MAE. For MLR, the improvement is almost neglectable.~~



587 **Figure 3: Split sampling results for the benchmark to-beat taken from WaterGAP2 (WG2) and different versions of**
 588 **the traditional regionalization methods: Multiple Linear Regression (MLR), Similarity Indices (SI) and Spatial Prox-**
 589 **imity (SP).**
 590

591 Thus, using only climatic descriptors—in our case, the mean temperature and information about radiation—is
 592 insufficient for regionalization. Instead, physiographic descriptors appear more critical for regionalization than the
 593 selected climatic descriptors. However, the best results are obtained when combining climatic and physiographic
 594 descriptors. Others often apply the combination of climatic and physiographic descriptors, leading to optimal re-
 595 gionalization results (e.g., Oudin et al., 2008; Reichl et al., 2009).

596 The reduced importance of climatic descriptors is surprising, as the climatic descriptors tend to have a higher
 597 information gain and correlation to the model parameter (see Table 1). Moreover, climatic information is often
 598 used as a central part of other regionalization studies, e.g., to assess regionalization (e.g., Parajka et al., 2013; Guo
 599 et al., 2020). One possible reason for this discrepancy in other studies is that we used pure meteorological data as
 600 climatic descriptors for the regionalization method. In contrast, others used derived information such as Köppen-
 601 Geiger climate zones or the Aridity Index (e.g., Beck et al., 2016; Yoshida et al., 2022).

602 When expanding the analysis to all descriptors, the performance changes slightly (i.e., mean MAE \pm 0.05).
 603 Thus, increasing the number of descriptors does not increase the performance of regionalization at some point (in
 604 line with Oudin et al., 2008 using a comparable Physical Similarity approach). This suggests that uncorrelated,
 605 non-redundant descriptors do not interfere with the regionalization using SI and MLR. Instead, a certain amount
 606 of information is beneficial to increase the regionalization method. After reaching this point, adding descriptors
 607 does not increase the performance, probably because all extractable information is already present in the given
 608 descriptors.

609 Using an ensemble of ten donor basins for the SI approach results in slightly better MAE values in most cases than
 610 applying a single donor basin (see Appendix B). More remarkably, the variation in the MAE values decreases
 611 significantly for all ensemble approaches (i.e., the reduction in standard deviation in MAEs is about 50%). Thus,
 612 introducing an ensemble approach for SI does not significantly improve the prediction performance. Still, it in-
 613 creases the likelihood that the prediction will perform well, i.e., be more robust. The positive effect of an ensemble
 614 approach for SI is already noted (Oudin et al., 2008). However, the literature-based number of donor basins might
 615 be adopted in future applications to be optimal for WaterGAP3, probably leading to higher performance.

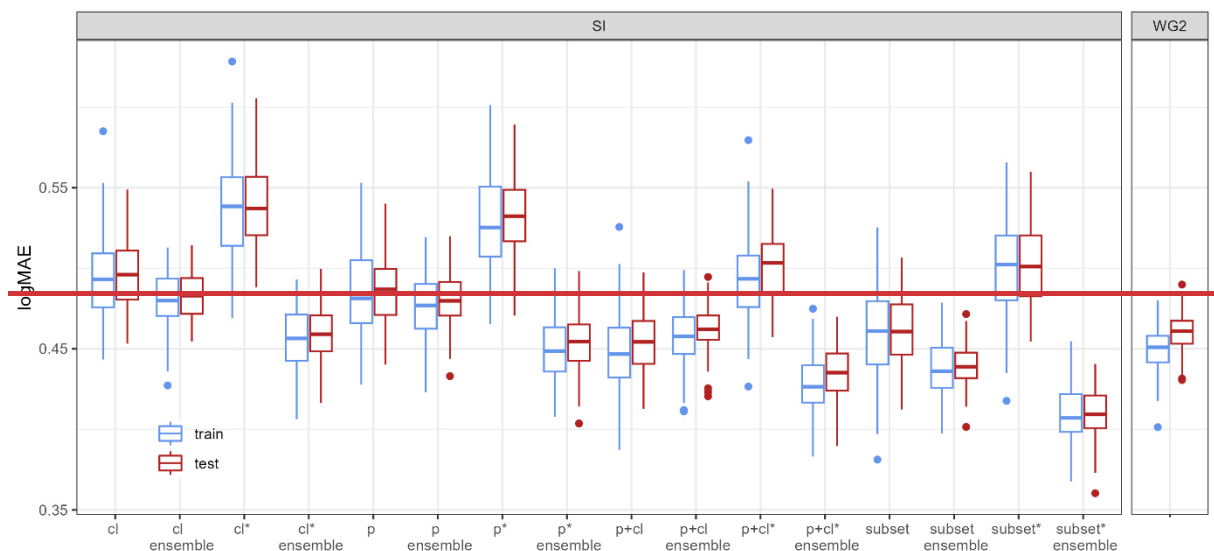
616 The introduction of tuning led to a significant increase in prediction performance for MLR, i.e., the median MAE
 617 for all MLR approaches improved by 0.04 (“cl”) and ~0.14 (others). For the ensemble-based SI approach, the
 618 tuning improves the median MAE by about 0.07 to 0.12. Thus, applying knowledge of the optimal parameter space
 619 enhances the quality of regionalization. This positive effect is not surprising, as incorporating a priori information
 620 about parameter distribution strengthens parameter estimation (e.g., described in Tang et al., 2016 using the Bayes
 621 Theorem).

622 The SP approach is the simplest applied, evaluating distances to the centroids without requiring regression or
 623 clustering. Thus, there is no training performance, only a testing performance. Applying the approach leads to a
 624 median MAE of 1.356, which is better than the benchmark to beat (median MAE in the testing of 1.544) and has
 625 the same quality as the best MLR and SI approaches without tuning (median MAE of 1.394 and 1.367, respec-
 626 tively). The good performance of SP is in accordance with other studies (e.g., Oudin et al., 2008; Qi et al., 2020).
 627 It indicates that this simple approach is suitable for WaterGAP3.

628 Nevertheless, the well-performing SP on a global scale is surprising as the distances between basins are potentially
 629 large and hydrological processes may strongly vary. It is probably beneficial for the SP approach that γ comprises
 630 all kinds of errors, e.g., spatially localised errors in global forcing products (e.g., Beck et al., 2017 reported errors
 631 for arid regions in the precipitation product) or inaccurately represented processes for larger regions. Thus, the
 632 estimation of γ might be appropriate, but not because of the same hydrological behaviour but due to the same kind
 633 of errors.

634 3.2 Evaluating Machine Learning-based Approaches

635 In this section, we assess whether machine learning-based approaches outperform the benchmark to beat and are
 636 suitable as a new regionalization method for WaterGAP3. We compare the ensemble of MAE for training and
 637 testing for RF and k-means with the benchmark to beat (see Fig. 4).



638 **Figure 4: Split sampling results for the benchmark to beat taken from WaterGAP2 (WG2) and different versions of**
 639 **machine learning-based approaches: k-means (in combination with k-NN) and Random Forest (RF).**
 640

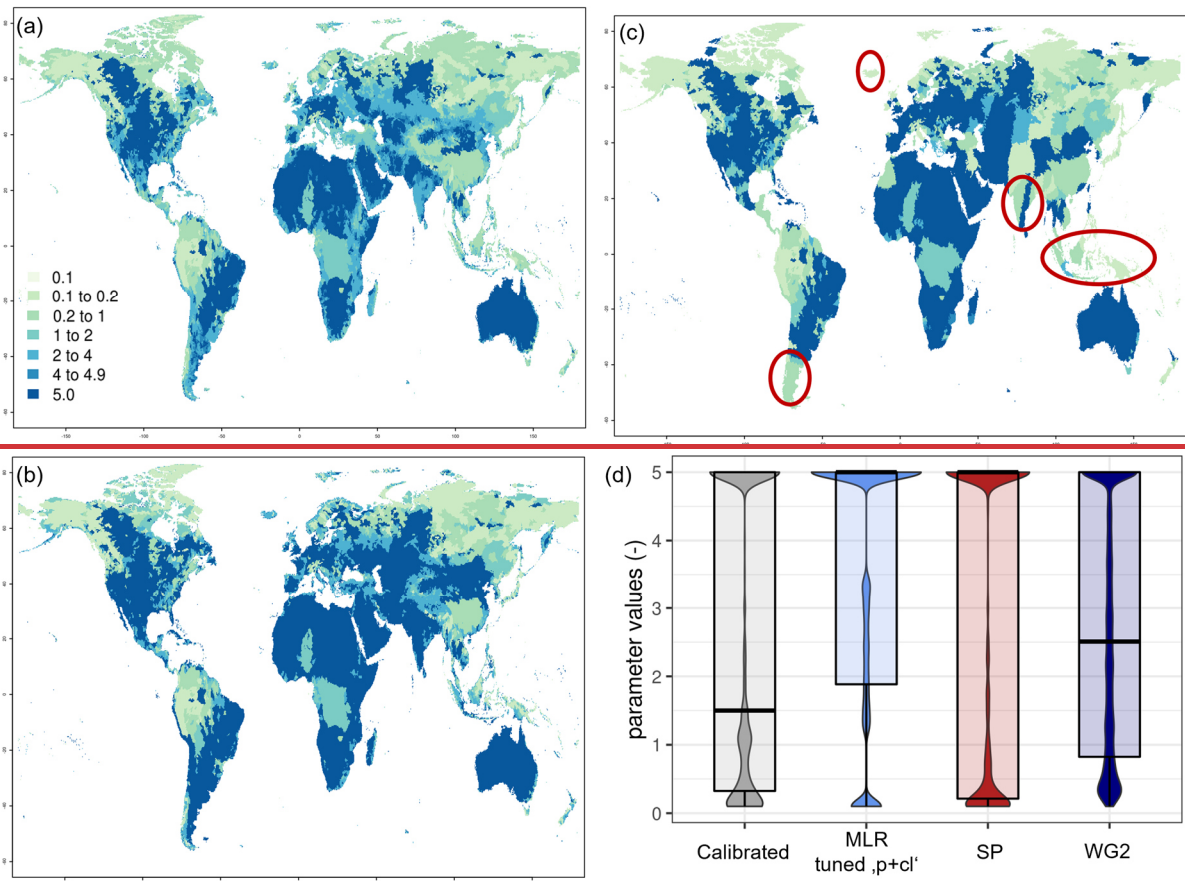
641 The RF approach is highly accurate within the training, i.e., fitting to calibrated γ values works well for gauged
 642 basins. However, it suffers a significant loss in performance when predicting the γ values for the pseudo-ungauged

643 basins. Although RF still has low MAE values in testing, the loss in performance from training to testing is signif-
644 icantly higher compared to other methods. This performance loss indicates that RF is not a robust regionalization
645 method for WaterGAP3. Other studies which reported good performance of RF in terms of regionalization have
646 not investigated the stability of the performance from training to testing (Golian et al., 2021; Wu et al., 2023).
647 Likely, the mathematical problem of predicting the calibrated parameter for WaterGAP3, with all its challenges
648 (e.g., tailored and heavy tailed parameter space, incorporation of many sources of errors), cannot be adequately
649 solved by RF. Thus, although RF is known to be especially robust among other machine learning based techniques,
650 it shows symptoms of over parameterization, meaning that the algorithm is too flexible and adjusts to noise in the
651 data, missing the underlying systematic. This lack of robustness is particularly disadvantageous since, for Wa-
652 terGAP3, regionalization is applied globally, requiring regionalizing large parts of the world.

653 The k means approach does not show such a performance loss between training and testing in almost all variants.
654 The only variant with comparable performance loss is the “highly flexible” k means approach. Interestingly, the
655 “highly flexible” k means approach was developed to emulate the same flexibility as in SI, which does not show
656 such performance loss between training and testing. This difference in robustness indicates that the applied k-
657 means algorithm does not extract the information from the descriptors as efficiently as the SI approach. The lack
658 of efficient data use for some clustering methods in the context of regionalization has already been reported by
659 Pagliero et al. (2019). This could also contribute to the presented the k means falling behind the benchmark to-
660 beat. Therefore, we conclude that the developed clustering is inappropriate for regionalizing WaterGAP3.

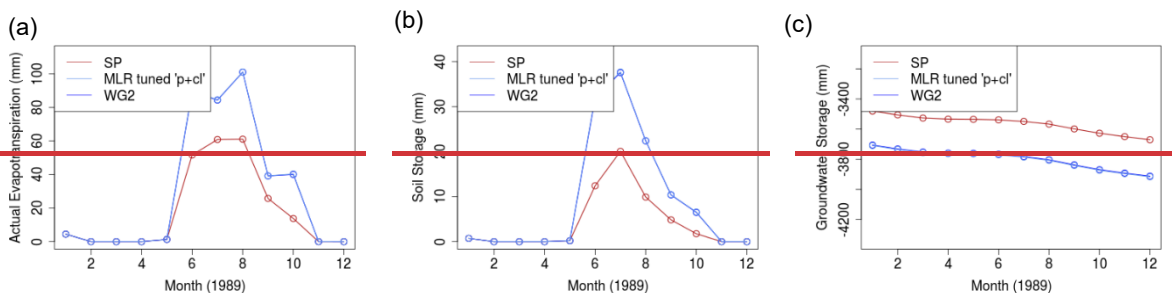
661 3.3 Implications of Regionalization

662 Finally, we highlight the possible implications of choosing regionalization methods for GHMs, where large parts
663 of the world need to be regionalized. For this purpose, a local analysis of internal states and fluxes and a continental
664 and global assessment of the water balance are undertaken. Therefore, we run WaterGAP3 from 1980 to 2016 with
665 different γ distributions. We choose two equally valid solutions for the regionalization of WaterGAP3 to produce
666 equally valid global γ distributions: (1) the SP approach because of its simplicity and because it outperforms our
667 benchmark to beat, and (2) the tuned MLR “p+cl” because it outperforms our benchmark to beat and its applica-
668 tion is very similar to the original regionalization approach of WaterGAP3. The tuned Similarity Indices “p+cl”
669 with an ensemble of 10 donor basins is also a valid solution for regionalizing γ . However, its application is more
670 complex than MLR and SP and differs considerably from the original WaterGAP3 regionalization. Therefore, it
671 has not been implemented and tested. In addition, we run the model with our benchmark to beat as it is our refer-
672 ence for assessing changes. We use the best performing benchmark to beat and MLR models out of the 100 trained
673 models for the analysis.



674
 675 **Figure 5: Global γ distribution for different regionalization methods, highlighting areas of differences (a) γ distribution**
 676 **using the MLR approach with parameter space tuning, using physiographic and climatic basin descriptors as independ-**
 677 **ent variables, i.e., tuned MLR “p+cl”, (b) benchmark to beat, WG2, (c) Spatial Proximity approach, i.e., SP and (d)**
 678 **global distribution of regionalized and calibrated parameter values.**

679 First, we compare the resulting global distribution of γ values for all three approaches (see Fig. 5). In particular,
 680 ungauged regions such as Indonesia, India and New Zealand exhibit significant differences in the predicted γ value.
 681 For these regions, the regionalized value varies depending on the methods used for regionalization. In contrast,
 682 ungauged areas such as North Africa do not differ much in regionalized values. Regionalization, therefore, appears
 683 to lead to a spatially varying uncertainty in ungauged regions. The differences in the regionalization methods also
 684 become apparent when comparing the resulting distribution of γ (see Fig. 5d). The approach MLR tuned “p+cl”
 685 tends to predict values at the upper bound more often than the other methods, which is probably due to the tuning
 686 within the method. The benchmark to beat approach from WaterGAP2 leads to a less heavy tailed prediction than
 687 others. The SP based approach shows the highest similarity to the distribution of the calibrated γ values.



688 **Figure 6: Differences in monthly internal states and fluxes of WaterGAP3 for one grid cell with varying regionalized**
 689 **value (SP: 0.325, MLR tuned “p+cl”: 5 and benchmark to beat (WG2): 4.467243), located in India**

(21.519794°|70.566733°) for a) actual evapotranspiration, b) soil storage and c) groundwater storage for 1989 as an exemplary year. Note that MLR tuned “p+cl” and WG2 are so close that they appear to be one line.

To highlight the impact of local differences in the parameter value, we examine an exemplary location in India where the regionalized values are 0.325, 5 and 4.467243 for SP, MLR tuned “p+cl” and the benchmark to beat, respectively. We show the resulting actual evapotranspiration (AET), the filling of the soil storage and the groundwater storage for one exemplary year (see Fig. 6). The internal states and fluxes from the MLR tuned “p+cl” and the benchmark to beat are not significantly different for all states, as the two lines are very close and appear to be one single line. However, there are considerable differences between the two MLR based approaches and SP, particularly in the amplitude of the AET and the soil storage. Acceleration effects cause the lower amplitudes for these two components. Reducing values of γ leads to a faster outflow of the soil storage, resulting in lower AET and soil moisture; additionally, smaller values of γ lead to higher groundwater storage due to accelerated percolation.

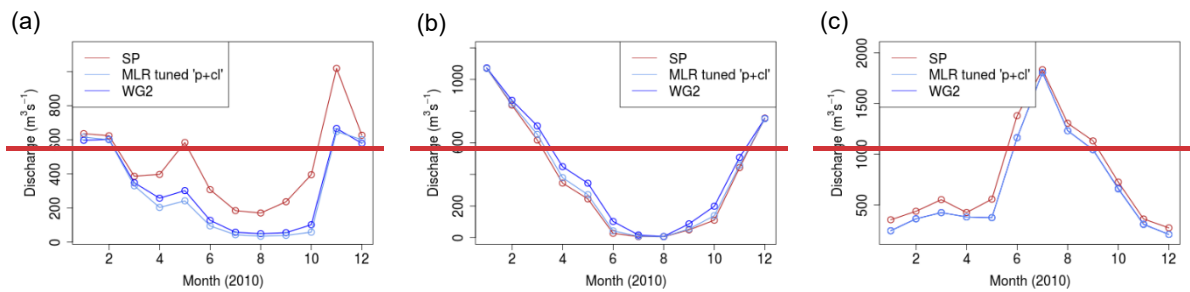


Figure 7: Simulated monthly runoff using three different regionalization methods for a) the Tiber, b) the Ebro and c) Rio Negro (in Argentina) for 2010 as an exemplary year.

Further on, we highlight the local effects of regionalization on discharge for the Tiber, the Ebro and Rio Negro for one exemplary year in Figure 7. Whereas the simulated discharge is higher for SP compared to the other methods in the Tiber and Rio Negro, the discharge is lower for the Ebro. Thus, one regionalization method does not always increase or decrease the discharge but results in locally varying effects on the water balance. Moreover, the similar results for MLR tuned “p+cl” and the benchmark to beat on the grid cell level (see Figure 6) propagate to a similar discharge pattern at the basin scale. Further, differences between SP and the other regionalization methods at the grid scale can lead to high differences at the basin scale, i.e., the simulated discharge of the Tiber is almost doubled for SP in May.

Finally, we evaluate how the observed variation due to different regionalization approaches propagates globally. Therefore, we assess the quantitative influence of regionalization by comparing a key component of the water balance, i.e., outflow to the ocean and inland sinks. Table 2 shows the resulting differences in the selected flow for all three model runs, aggregated to continental and global scales. The results highlight that the differences in mean annual outflow vary spatially and between the regionalization methods. The results of SP differ significantly from the two MLR based approaches in some parts of the world. In Oceania, the SP approach exhibits a deviation of 7.7 % in the selected flow compared to the benchmark to beat. This difference may be attributed to the significant disparity in γ between the two methods in New Zealand (see Fig. 5).

Table 2: Mean outflow to the ocean and inland sinks in $\text{km}^3 \text{yr}^{-1}$ between 1980–2010

Continent	benchmark-to-beat	MLR	SP
Africa	5005.10	0.972	0.968
Asia	15977.39	1.005	1.114
Oceania	1188.42	0.977	0.923
Europe	3028.47	0.981	1.030
South America	11612.39	0.997	1.039
North America	7283.21	0.994	1.025
Global	44094.97	43876.01	46456.35

722

723 Similarly, SP exhibits a high deviation of 11.4 % in the mean outflow in Asia, which is likely due to the varia-
724 tion of γ in India (see Fig. 5). In contrast, the southern part of South America, which shows a relatively high de-
725 viation in γ , does not lead to a significant deviation in the mean outflow for the continent. This limited impact of
726 varying parameter values in southern South America may be attributed to the lower water availability in this re-
727 gion, which only slightly affects the continental water balance. These results suggest that the impact of regionali-
728 zation methods on the continental water balance depends on (1) the variation in predicted parameter values and
729 (2) the region's sensitivity to the water balance. Examining the global estimates, the differences between the
730 benchmark-to-beat and SP results in approximately $2400 \text{ km}^3 \text{ yr}^{-1}$ which is in the range of inter-model differ-
731 ences (see Table 2 in Widen Nilsson et al., 2007).

732 Although the two newly developed methods performed similarly during the split sample test, significant differ-
733 ences were observed when simulating the water balance. It was expected that the methods MLR tuned “p+cl”
734 and SP methods would differ less due to their similar performance during the split sample tests. However, it be-
735 came apparent that the two MLR based methods resulted in more closely simulation results than the SP based
736 approach. This indicates that the method selection, such as spatial proximity based or regression based, has a
737 greater influence on the regionalization than the details of executing the method. Moreover, the split sample test
738 should be extended to get deeper insights into the method's robustness. For example, the SP and SI robustness
739 check could be extended by the so-called “HDes” approach, which Lebecherel et al. (2016) recommended. In
740 this approach, the closest basin to the corresponding (pseudo-) ungauged basin would be ignored during the re-
741 gionalization to measure the robustness of the regionalization method.

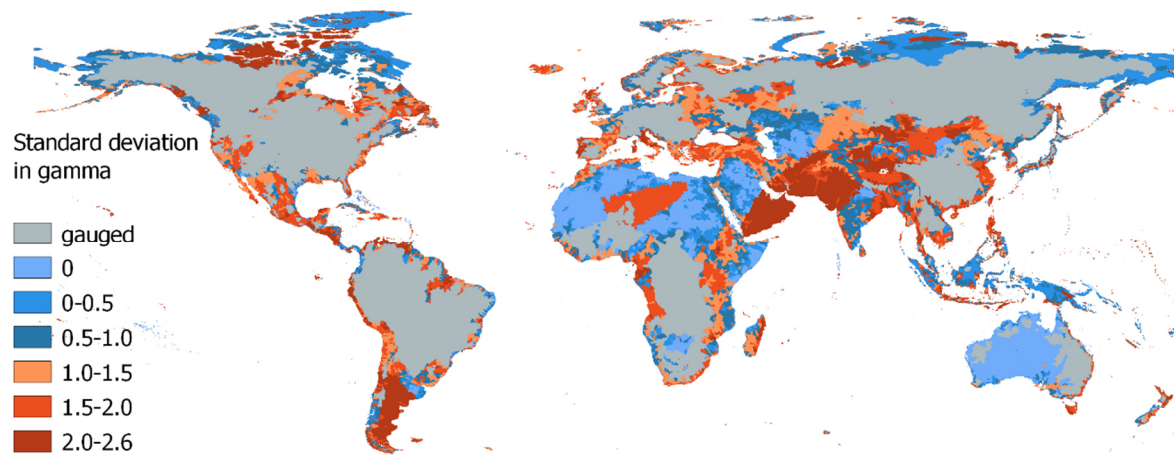
742 **3.4 Impacts on runoff simulations**

743 To evaluate the impact of runoff simulations, we apply an ensemble of regionalization methods generating γ esti-
744 mates for the worldwide ungauged regions. Within the ensemble, we use the four methods SI (best), knn (best),
745 MLR (best), and SP that (1) outperform the benchmark-to-beat regarding the logMAE of regionalized and cali-
746 brated values and (2) perform similarly to each other and better than the benchmark-to-beat in KGE for monthly
747 discharge. Additionally, we use the benchmark-to-beat as the fifth member of our regionalization method ensem-
748 ble. The entire set of 933 gauged basins is used for regionalizing γ , resulting in five distinct worldwide distributions
749 of γ . The spatially distributed standard deviation of the regionalized values is shown in Fig. 5.

750 In particular, the southern parts of South America, the northern and southern parts of North America, and Central
751 Asia reveal differences in γ across the ensemble of regionalization methods (see Fig. 5). In Europe, the highest

752 differences in regionalized values are observed in Italy, Great Britain, and northern Portugal. In Oceania, the high-
753 est values in standard deviation of γ are in Tasmania, New Zealand, and the southwest of Australia's coast. In
754 contrast, a minor variation in γ is apparent in northern Africa, most parts of Australia, and the East of the Dead
755 Sea. Thus, the uncertainty associated with globally regionalizing γ seem to vary across different regions.

756 4. Cone



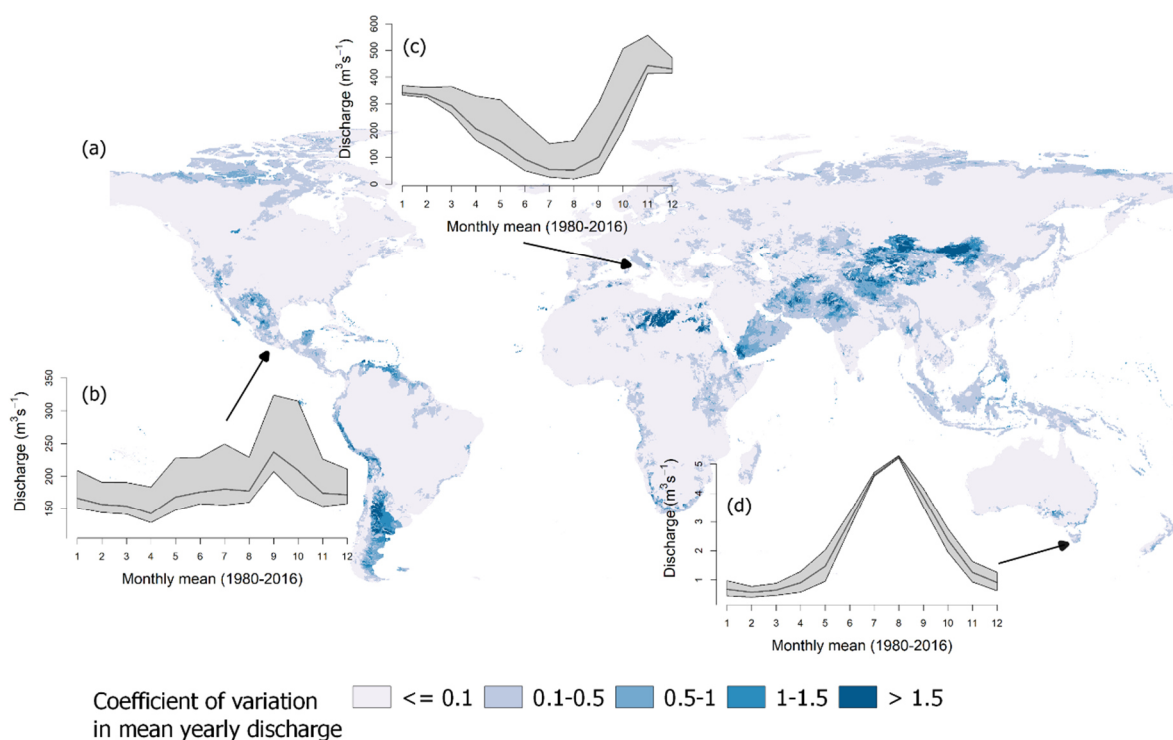
757 Figure 5: Standard deviation in regionalized γ values using the best approaches of MLR (best), SI (best), SP, knn (best),
758 and the benchmark-to-beat. Note that dry regions without discharge are set to zero.

760 An example of how these uncertainties in regionalized values propagate through the water system is presented in
761 Fig. 6. This figure displays the coefficient of variation of the mean yearly discharge between 1980 and 2016 based
762 on the five simulation runs. Moreover, we highlight the effect on rivers in ungauged regions by showing the re-
763 sulting seasonal pattern, i.e., the simulated long-term mean of monthly river discharge for three exemplary rivers.
764 These rivers are the Río Bravo in Mexico, the Tiber in Italy, and the Tamar River in Tasmania. Each river is located
765 in an ungauged region, where the standard deviation in γ is high (see Fig. 5).

766 Comparing Fig. 5 and Fig. 6 reveals that regions showing variability in γ tend to exhibit variation in mean yearly
767 discharge. However, the impact of variation in γ on the simulated discharge appears to vary spatially. Some regions
768 showing a high degree of variation in γ do not exhibit a correspondingly high degree of variation in discharge. For
769 example, 45 % of all ungauged regions showing a low variation in discharge, i.e., the coefficient of variation is
770 below 0.5, exhibit a standard deviation of more than one in γ . In contrast, about 89 % of the ungauged regions
771 showing a higher discharge variation exhibit a standard deviation of more than one in γ . Thus, variation in γ does
772 not necessarily lead to variation in river discharge, but it increases the likelihood that a region's discharge is af-
773 ected. The spatially varying impact of γ is likely related to varying sensitivity regarding γ in the ungauged regions,
774 which depends on numerous aspects, e.g., snow occurrence or waterbodies (see Kupzig et al., 2023).

775 About 11 % of the ungauged area exhibits variations in yearly river discharge exceeding 50 % of the mean. These
776 regions are primarily in southern South America and Central Asia. A further 62 % of the ungauged area exhibits
777 variations in yearly river discharge between 10 % and 50 % of the mean. These regions are mainly located on the
778 northern coast of Russia and northern Canada, Indonesia, and Tasmania. Other areas, like most ungauged regions
779 of Africa and Australia, show almost no impact, i.e., the variation in yearly discharge is less than 10 % of the
780 mean. In northern Africa, one region exhibits higher values in the coefficients of variation. These values are at-
781 tributable to minimal discharge values, resulting in comparatively high coefficients of variation in this region.

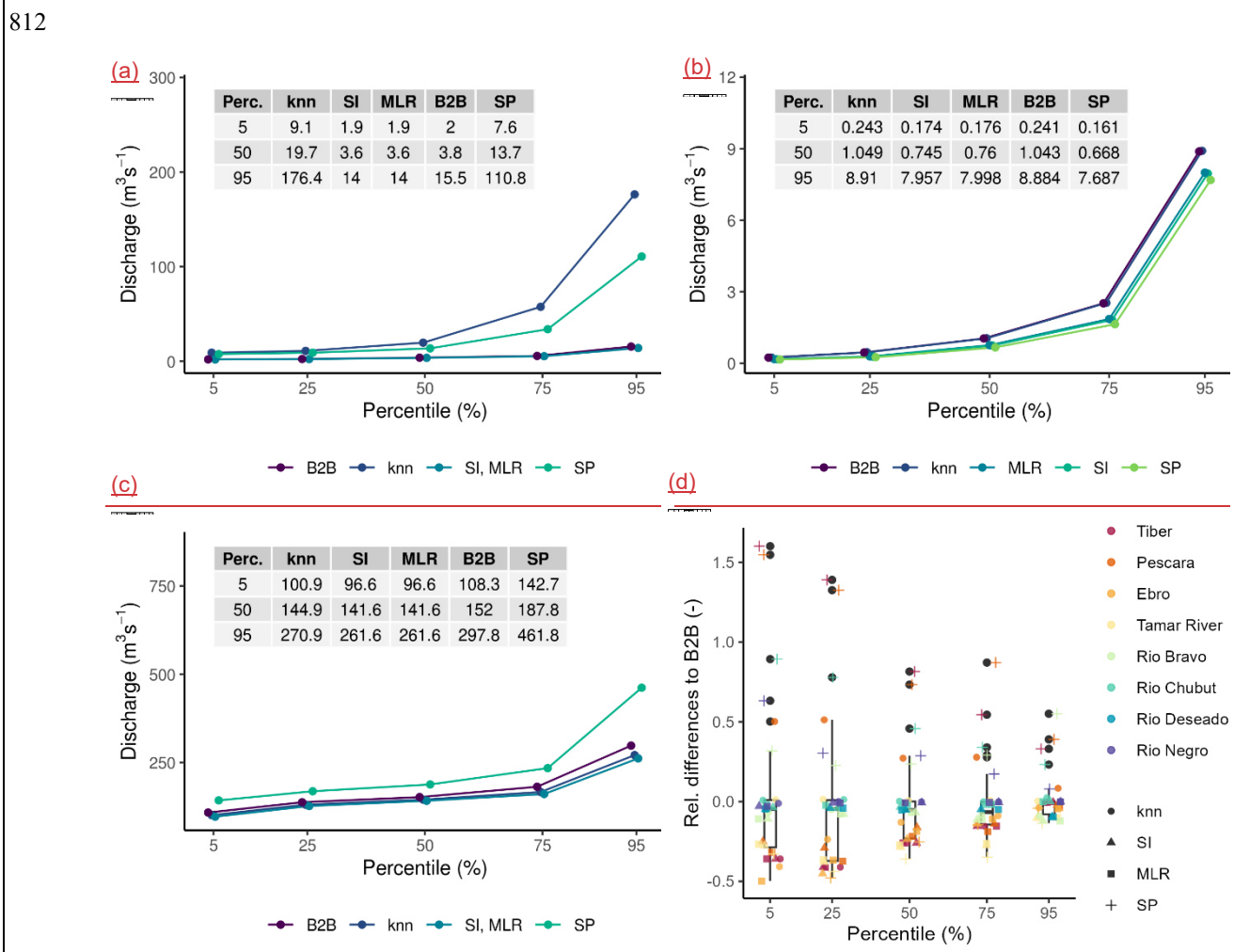
782 Considering the variation in the seasonality in the selected ungauged river systems (see Fig. 6b-d), the temporal
 783 impact of regionalization varies across the local landscape. For the Tamar River in Tasmania, as illustrated in Fig.
 784 6d, the variation is higher at the start and end of the dry periods in October/November and April/May, respectively.
 785 The spread in monthly mean discharge is about $0.7 \text{ m}^3\text{s}^{-1}$ to $1 \text{ m}^3\text{s}^{-1}$ in these periods. The Tiber in Italy and the Río
 786 Bravo in Mexico exhibit a similar pattern: using the regionalized γ values of SP leads to much higher discharge
 787 rates than other ensemble members, introducing broad uncertainty bands. For the Tiber, this leads to seasonal
 788 estimates varying between 1.2 % (in January) and 11 % (in October) of the mean yearly sum. The Río Bravo shows
 789 variations in its seasonal pattern, with values ranging from 2.2 % (in February) to 6.8 % (in October) of the mean
 790 yearly sum. Thus, all rivers display a temporally varying impact. Whereas the main variation in the discharge of
 791 the Río Bravo and the Tiber is mainly attributed to the SP regionalization run, for the Tamaris River, all regional-
 792 ization runs contribute to the varying long-term monthly mean in discharge.
 793



795 **Figure 6: a) Global map of the coefficient of variation in mean yearly discharge for the applied regionalization methods.**
 796 **Resulting differences in the regionalization ensemble regarding the long-term mean of monthly discharge are depicted**
 797 **for: b) the Río Bravo in Mexico, c) the Tiber in Italy and d) the Tamar River in Tasmania. The grey-shaded area**
 798 **indicates the range of the long-term mean of monthly discharge and the black line indicates the mean off all simulation**
 799 **runs.**

800 To gain a deeper understanding of the local impact of regionalization on runoff simulations, we analyze the annual
 801 percentiles from 1980 to 2016 for Río Deseado in Argentina, Río Bravo, and Tamar River, displaying the mean
 802 percentile of all years (see Fig. 7a-c). As the Tiber and Río Bravo display high similarities in the resulting patterns
 803 of percentiles, we demonstrate the impact by showing the percentiles from the Río Bravo. Additionally, we com-
 804 pare the relative differences in the mean for each percentile using eight ungauged river systems (see Fig. 7d), as
 805 previously done by Gudmundsson et al. (2012) for nine GHMs. To calculate the relative difference, we subtract
 806 the mean annual percentile of a method from the corresponding mean annual percentile of the reference and divide
 807 the resulting difference by the mean annual percentile of the reference. Instead of using observed flow as a refer-
 808 ence, we use the annual percentiles of our benchmark-to-beat. As river discharge is already spatially aggregated

809 information, it is unnecessary to spatially aggregate grid cells to create results comparable to those of Gudmunds-
 810 son et al. (2012), who used cell runoff. The evaluated river systems are Río Chubut, Río Deseado, Río Negro, Río
 811 Bravo, Tamar River, Tiber, Pescara, and Ebro.



813 **Figure 7: Mean annual percentiles between 1980 and 2016 of simulated discharge using an ensemble of regionalization**
 814 **methods. The river are a) Río Deseado, b) Tamar River, and c) Río Bravo. In d), the relative differences in mean annual**
 815 **percentiles to the benchmark-to-beat of eight ungauged river systems are presented. Negative values indicate smaller**
 816 **mean annual percentiles than the benchmark-to-beat. Note that all data points from Río Deseado for knn and SP are**
 817 **excluded as the values are above 2.0.**

818 In Fig. 7a, Río Deseado is highly affected by uncertainties in simulated discharge due to the different regionaliza-
 819 tion methods; all segments of the percentiles show high variations where the absolute spread is increasing with
 820 increasing percentiles. For SP and knn (best), the discharge is highest, e.g., estimating a median discharge of 13.7
 821 m³s⁻¹ and 19.7 m³s⁻¹, respectively. For the other methods, the simulated discharge is low, e.g., SI and MLR result
 822 in an equal median discharge of 3.6 m³s⁻¹. The Tamar River in Fig. 7b also shows increasing absolute differences
 823 between the methods for higher percentiles, with the benchmark-to-beat approach leading to the highest discharge.
 824 For the Río Bravo, the absolute differences between the highest result of SP and the other methods remain almost
 825 constant until the 75th percentile. For the 95th percentile, the absolute differences increase rapidly from about 40
 826 m³s⁻¹ (75th percentile) to nearly 200 m³s⁻¹ (95th percentile). The exemplary results of Río Deseado and Río Bravo
 827 indicate a potentially high degree of uncertainty regarding the high percentiles in discharge simulation. These
 828 uncertainties put the results of global flood frequency analysis (e.g., Ward et al., 2013) in ungauged regions at risk

829 as the time series of annual maxima might be even more uncertain. Thus, the results of flood frequency analysis
830 should be carefully interpreted in ungauged regions as the impact of parameter regionalization may be significant.
831 Upon examination of the relative differences to the benchmark-to-beat for eight ungauged river systems, it be-
832 comes evident that the impact of regionalization methods varies between ungauged river systems (e.g., Río Negro
833 exhibits almost no variation, but Ebro does). Moreover, it becomes apparent that some regionalization methods
834 contribute more to the variation in estimated discharge than others. The methods contributing most are knn (best)
835 and SP. For knn (best), 10 of the 40 relative differences are higher than |0.3|. For SP, even 29 out of the 40 relative
836 differences are higher than |0.3|. The results of SI (best) and MLR (best) are very similar, indicating high similarity
837 in performance. This is consistent with the KGE evaluation (see Chapter 3.3), in which they performed similarly.
838 The observation in Fig. 7d that higher relative differences of discharge simulations occur in drier percentiles is
839 also reported in Gudmundsson et al. (2012). Moreover, the relative differences between the five regionalization
840 runs seem comparable to the inter-model differences depicted in Gudmundsson et al. (2012), indicating the high
841 impact of regionalization methods on the evaluated ungauged river systems.

842 Finally, Table 3 presents the estimated yearly mean runoff to the ocean for all five ensemble members. All esti-
843 mates of global "runoff to ocean" range from 45,622 (SI (best)) to 47,069 (SP). Thus, the differences are on the
844 scale of smaller inter-model differences (see Table 2 in Widen-Nilsson et al., 2007). The impact of regionalization
845 becomes even more evident using an unsuitable regionalization method for WaterGAP3. For instance, the tuned
846 kmeans ("subset") approach results in 42,862 km³ yr⁻¹ "runoff to ocean", increasing the spread between the meth-
847 ods to 4,208 km³ yr⁻¹ being in the scale of inter-model differences. This high impact of regionalization on global
848 "runoff to ocean" is surprising, given that only 27 % of the world is ungauged, using the GRDC database. From
849 this 27 %, most regions are in Australia and Africa, where minimal runoff is produced. In studies employing
850 disparate models, e.g., for inter-model comparison, all regions are simulated in disparate ways.

851 The most significant deviations in the continental sums of "runoff to ocean" in Table 3 are due to SP. Only for
852 Europe is the highest deviation related to MLR (best), not SP. Interestingly, the estimated sums of SP occasionally
853 define the lowest and occasionally the highest extremes for the continents, lacking a systematic pattern. The out-
854 standing role of SP is consistent with previous evaluations in this Chapter, where SP frequently contributes most
855 to the variation in discharge. This suggests that SP may not be suitable for the global scale. Nevertheless, the
856 pseudo-ungauged basins in the split-sample tests may also exhibit considerable distances from the observed basins.
857 Given that SP achieved satisfactory results in both evaluations, using either the logMAE or the KGE, the evaluation
858 indicates the method's suitability on a global scale. Thus, in the future, the split-sample test must be extended to
859 gain deeper insights into the method's robustness and make a definitive statement about the method's suitability
860 on a global scale. For example, the so-called "HDes" approach, recommended by Lebecherel et al. (2016), could
861 be applied for this purpose. In this approach, the closest basin to the corresponding (pseudo-) ungauged basin is
862 excluded from the regionalization process, thereby enabling an assessment of the method's robustness.

863 **Table 3: Mean outflow to the ocean and endorheic basins in km³ yr⁻¹ between 1980-2016. The highest continental devi-**
864 **ation to the benchmark-to-beat is indicated in bold.**

<i>Runoff to ocean¹</i>	B2B	SI (best)	knn (best)	MLR (best)	SP
<u>Oceania</u>	1,127	-1.80 %	-2.20 %	-3.40 %	-6.60 %
<u>Europe</u>	3,098	-2.30 %	-0.10 %	-2.60 %	0.20%
<u>Asia</u>	16,676	3.50 %	0.30 %	1.60 %	5.50 %

<u>Africa</u>	<u>5,203</u>	<u>-1.00 %</u>	<u>0.70 %</u>	<u>-0.30 %</u>	<u>-3.60 %</u>
<u>North America</u>	<u>7,517</u>	<u>0.30 %</u>	<u>1.00 %</u>	<u>-1.70 %</u>	<u>2.20 %</u>
<u>South America</u>	<u>12,032</u>	<u>1.30 %</u>	<u>1.40 %</u>	<u>-0.20 %</u>	<u>4.90 %</u>
<u>global</u>	<u>45,653</u>	<u>46,273</u>	<u>45,953</u>	<u>45,622</u>	<u>47,069</u>

¹including endorheic basin

865 **Conclusion**

866 Valid simulation results from GHMs, such as WaterGAP3, are crucial for detecting hotspots or studying patterns
867 in climate change impacts. However, the lack of worldwide monitoring data makes adapting GHMs' parameters
868 for valid global simulations challenging. Therefore, regionalization is necessary to estimate parameters in un-
869 gauged basins. This study applies regionalization methods for the first time to WaterGAP3, aiming to provide
870 insights into selecting suitable regionalization methods and evaluating their impact on the runoff simulations. Tra-
871 ditional and machine learning-based methods are tested to assess the application of several regionalization tech-
872 niques on a global scale. The concept of benchmark-to-beat and an ensemble of split-sampling tests are employed
873 for a comprehensive evaluation. Moreover, the impact on runoff simulation is assessed using a wide range of
874 temporal and spatial scales, i.e., from the daily to the yearly and from the local to the global scale.~~Valid simulation~~
875 ~~results from GHMs, such as WaterGAP3, are crucial for detecting hotspots or studying patterns in climate change~~
876 ~~impacts. However, the lack of worldwide monitoring data makes adapting GHMs' parameters for valid global~~
877 ~~simulations challenging. Therefore, regionalization is necessary to estimate parameters in ungauged basins. This~~
878 ~~study introduces novel regionalization methods for WaterGAP3 and aims to provide insights into selecting a suit-~~
879 ~~able regionalization method and evaluating its impact on the simulation results. Traditional and machine learning-~~
880 ~~based methods are tested to assess the advantages of using new techniques on a global scale. The concept of~~
881 ~~benchmark to beat and an ensemble of split sampling tests are employed for a comprehensive evaluation.~~

882 In this study, four regionalization methods outperform the benchmark-to-beat and thus are considered appropriate
883 for WaterGAP3. These methods span the complete range of methodologies, i.e., regression-based methods and
884 methods using the concept of physical similarity and spatial proximity. Moreover, the methods vary in the de-
885 scriptors used to achieve optimal results. This highlights that different methods use descriptor sets with varying
886 efficiency. All methods perform best when using climatic and physiographic descriptors, indicating that combining
887 climatic and physiographic descriptors is optimal for regionalizing worldwide basins. Although random forest is
888 known to be especially robust among other machine learning-based techniques, it shows symptoms of over-pa-
889 rameterization, indicating that the algorithm is too flexible and adjusts to noise in the data, missing the underlying
890 systematic pattern.

891 Our results demonstrate that variation in the regionalized parameter value does not necessarily lead to variation in
892 river discharge. However, it increases the likelihood that a region's runoff is affected. This spatially varying impact
893 of γ is likely related to the varying sensitivity in ungauged regions regarding γ . Southern South America is a region
894 identified to be especially sensitive to variation in γ . Furthermore, local effects on runoff simulations indicate a
895 temporally varying impact. For example, some impacted rivers indicate a high degree of uncertainty regarding the
896 high percentiles in discharge simulation. These uncertainties potentially lead to a significant impact on flood fre-
897 quency analysis on a global scale, where the lack of gauging stations in certain regions calls for regionalization.
898 The global impact of regionalization methods that perform well for WaterGAP3 appears to be in the order of minor

899 inter-model differences. This impact rigorously increases when using a poorly performing method for WaterGAP3,
900 underscoring the importance of carefully selecting regionalization methods.

901 The spatial proximity approach contributes most to the variation in estimated runoff. The outstanding role of this
902 approach suggests that it may not be suitable for the global scale. However, as the pseudo-ungauged basins in the
903 split-sample tests may also have considerable large distances to the observed basins, and the method achieves
904 satisfactory results in all executed evaluations, it is not possible to make a definite statement about the method's
905 suitability for the global scale. Further research is required to gain deeper insights into the methods' robustness,
906 e.g., by extending the analysis by applying the recommended "HDes" approach (Lebecherel et al., 2016).

907 Our results suggest that the basin-descriptor selection may not be crucial for regionalization in WaterGAP3 as long
908 as a subset of the selected descriptors contains relevant information. Additionally, introducing an ensemble ap-
909 proach for Similarity Indices does not necessarily improve the prediction performance but increases the likelihood
910 of robust predictions. Interestingly, the simplest regionalization method (using the concept of spatial proximity)
911 outperforms most of the developed regionalization methods and the benchmark to beat. In contrast, the more com-
912 plex, machine learning-based approaches deliver insufficient prediction performance. The inadequate performance
913 may be attributed to an inefficient extraction of available information content from the descriptors and the blurring
914 relationship between the calibration parameter and basin descriptors, which is caused by including multiple error
915 sources in the calibration parameter values. This blurring relationship probably poses a high risk of over parame-
916 terization, which hinders the use of more flexible machine learning-based approaches.

917 Regionalization appears to result in spatially varying uncertainty for ungauged regions, with India and Indonesia
918 being particularly affected by higher uncertainty. The local impacts of regionalization in ungauged areas propagate
919 to the global scale, where the water balance component "outflow to the ocean and inland sinks" changed by about
920 2400 km³ yr⁻¹, which is in the scale of inter-model differences. As the selected regionalization method influences
921 the regionalization more than details on the execution of the method, we recommend employing simulation runs
922 that use multiple regionalization methods to account for the uncertainty induced by the chosen regionalization
923 method. Considering the uncertainty induced by regionalization is especially important when analysing regions
924 with a significant proportion of ungauged basins or high sensitivity to the examined target.

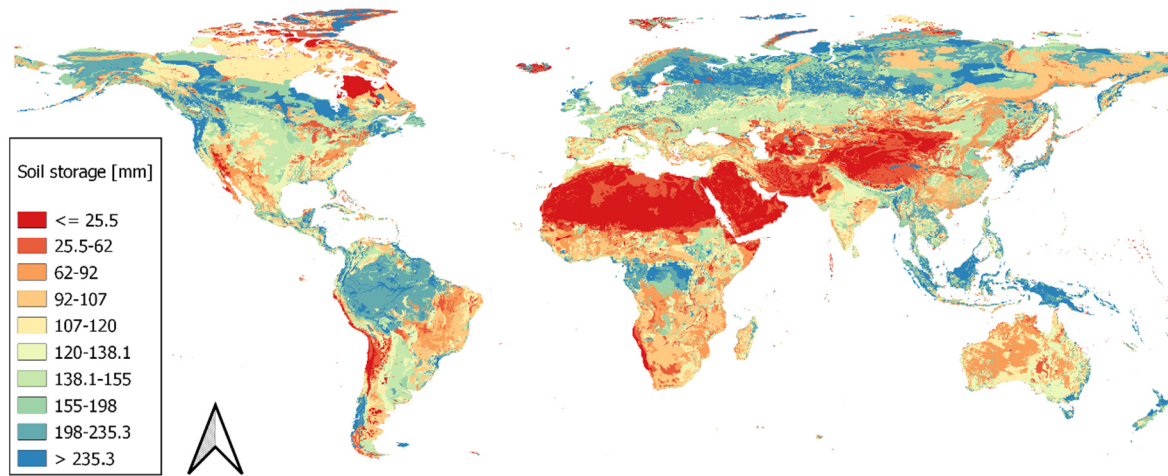
925 *Code and data availability.* The data and the supporting R-Code to reproduce this study's findings are available at
926 <https://doi.org/10.5281/zenodo.11833447> DOI:10.5281/zenodo.10803089.

927 *Authors contribution.* JK developed, designed, and drafted the study. NK helped to design the experiment. MF
928 provided feedback throughout the entire process and supported the writing.

929 *Competing interests.* The authors declare that they have no conflict of interest.

930

Appendix A: Global Map of derived global soil moisture storage



931

932

933

Figure A1: Global map of the size of soil storage based on Batjes (2012) and land use information (derived from Friedl & Sulla-Menashe, 2019)

934

Appendix B: Further analysis regarding the clustering of parameter values at the extremes

The clustered calibrated parameter values at the extremes of the valid parameter space (see Fig. 1b) are a known problem within the calibration. As the parameter space, i.e., the parameter bounds, is crucial for calibration and, in consequence, for regionalization, we address this issue by a brief sensitivity analysis to demonstrate that the clustering of the calibrated parameter values is more an issue of missing processes (or using additional parameter values) than an issue of inappropriate parameter space. As the lower limit of the calibrated parameter (0.1) is sufficiently small in comparison to other studies using a similar HBV-based approach for runoff generation processes (e.g., see the beta in Table A2 in Jansen et al., 2022), we focus on the sensitivity analysis on the upper limit of γ (5.0).

In the sensitivity analysis regarding the upper limit of γ , we applied the model formula (see equation B1) containing the model's parameter γ and modified it within the bounds of 0.1 and 10. Additionally, we modified the soil saturation varying from 1 % to 95 %.

$$\text{outflow} = \text{precipitation}_{\text{effective}} \cdot \text{soil saturation}^{\gamma} \tag{B1}$$

The calculated outflow and its relationship to the soil saturation and γ are depicted in Fig. B1 and B2. The incoming effective precipitation is defined as constant. As it is a factor in equation B1., the results regarding incoming effective precipitation are linearly scalable.

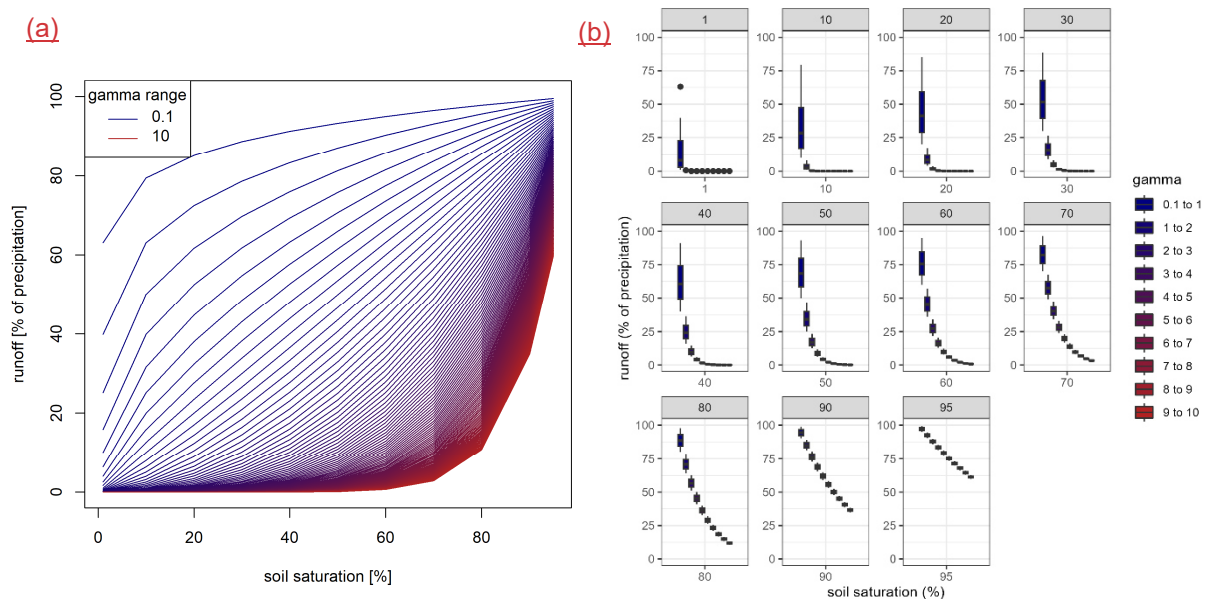


Figure B1: a) Runoff generation in the soil layer (neglecting overflow and evapotranspiration) using different values for the calibration parameter and increasing the soil-moisture, b) runoff generation for varying soil moisture grouped in bins of size one.

In the depicted Fig. B1, the runoff generation process differences between differing γ values become more linear when soil saturation increases. Thus, the non-linear model parameter becomes less critical for high soil moisture. Generally, the runoff generation process differences for higher γ values are more pronounced for higher soil moisture. For lower soil moisture, the smaller values have higher effects on the generated runoff. For example, for 70 % soil moisture, the differences for γ values ranging from 5 to 10 are between 3 % and 16 %. For the same soil moisture, the range in runoff generation varies from 16 % to 70 % for γ values between 1 and 5.

959 High γ values usually occur in dry regions (see Fig. 4b in Müller Schmied et al., 2021). In dry regions, high soil
960 moisture values are not expected to occur frequently (e.g., see Khosa et al., 2020; Oloruntoba et al., 2024 for
961 estimated and measured soil moisture in Africa and Draper et al., 2008 for estimated and measured soil moisture
962 in Australia). It is, therefore, unlikely that higher γ values will significantly enhance the calibration result or de-
963 crease the issue of clustered calibrated parameter values at the higher end of the parameter space. More likely, the
964 clustering of calibrated parameter values will be resolved in dry regions by incorporating additional (missing)
965 model processes, such as evaporation from rivers or inaccurate representation of groundwater processes (Eisner,
966 2016, p. 49). Thus, the parameter bounds of γ (e.g., also used in Eisner 2016, p. 16; Müller Schmied et al., 2021;
967 Müller Schmied et al., 2023) are not changed in this study.

968 Appendix CA: Basin descriptors

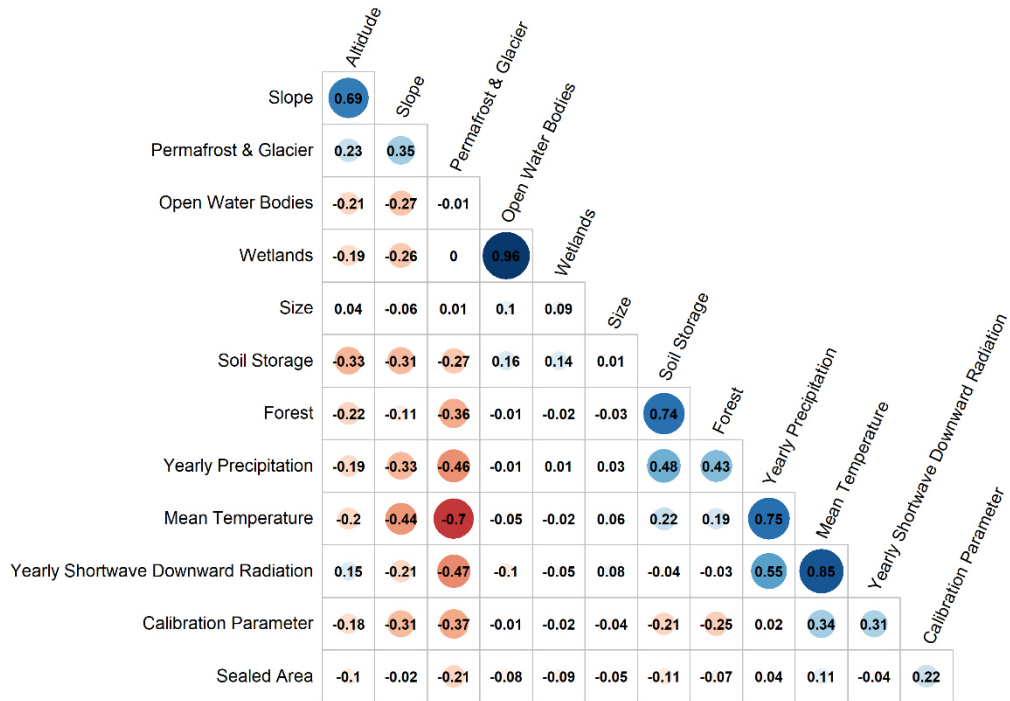
969 Overview of basins descriptors used in this study. All basin descriptors are derived from the original model input
970 and aggregated with a simple mean method to basin values to produce the same spatial resolution as the calibrated
971 model parameter.

- 972 • *Soil Storage*: The size of the soil storage, i.e., the maximal water content in the soil reachable for plants
973 in millimetresmm. The information is the product of rooting depth (defined in a look-up table) and the
974 total available water content derived from Batjes (20123).
- 975 • *Open Water Bodies*: The fraction of the area covered with open water bodies in the basin is given as a
976 percentage. The model input is based on the GLWD database (Lehner & Döll, 2004).
- 977 • *Wetlands*: The fraction of area covered with wetlands in a basin is given in percentage. The model input
978 is based on the GLWD database (Lehner & Döll, 2004).
- 979 • *Size*: Size of a basin in km².
- 980 • *Slope*: The mean slope class is calculated as described in Döll & Fiedler (2008) and based on GTOPO30
981 (USGS EROS data centre).
- 982 • *Altitude*: The mean altitude of a basin is given in metres-meters above sea level and based on GTOPO30
983 (USGS EROS data centre).
- 984 • *Forest*: The mean fraction of the area covered with forest is given in percentage and derived from MODIS
985 data (Friedl & Sulla-Menashe, 2019), where 2001 is used as a reference. All grid cells having a dominant
986 International Geosphere-Biosphere Programme (IGBP) classification between one and five are defined
987 as "_forest".
- 988 • *Sealed Area*: The mean fraction of sealed area is given in percentage and derived from MODIS data
989 (Friedl & Sulla-Menashe, 2019), where 2001 is used as a reference. All grid cells having an IGBP clas-
990 sification equal to 13 are defined as they would contain 60% of the sealed area. Note: The different treat-
991 ment of forest and sealed area is based on the required model input; whereas the land cover is a classified
992 value, the sealed area is a floating-point value.
- 993 • *Permafrost & Glacier*: The mean coverage of permafrost and glacier in a basin is given in percentage. It
994 is based on the World Glacier Inventory and the Circum-Arctic Map of Permafrost and Ground-Ice Con-
995 ditions.
- 996 • *Mean Temperature*: The mean air temperature is based on the meteorological forcing used to drive the
997 model (Lange, 2019) covering the period 1979 to 2016 and given in degrees Celsius.
- 998 • *Yearly Precipitation*: The yearly precipitation sum is based on the meteorological forcing used to drive
999 the model (Lange, 2019) covering the period 1979 to 2016 and given in millimetresmm.
- 1000 • *Yearly Shortwave Downward Radiation*: The yearly shortwave downward radiation is based on the me-
1001 teorological forcing used to drive the model (Lange, 2019) covering the period 1979 to 2016 and given
1002 in Wm⁻².

1003

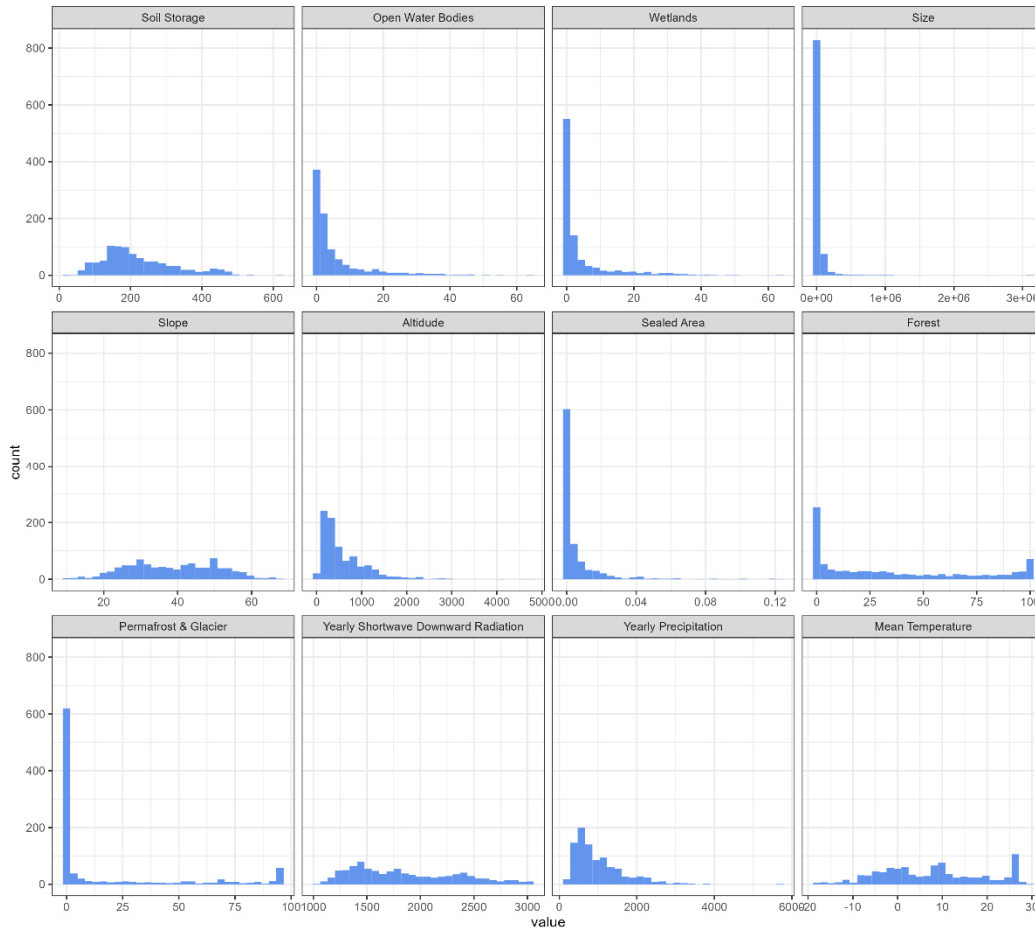
1004 The correlation between the defined basin descriptors is shown in Fig. A1. The variation within each basin de-
1005 scriptor for basins used for regionalization-regionalization is shown in Fig. A2.

1006



1007
1008
1009
1010

Figure CA1: Correlation between basins descriptors.



1011
1012

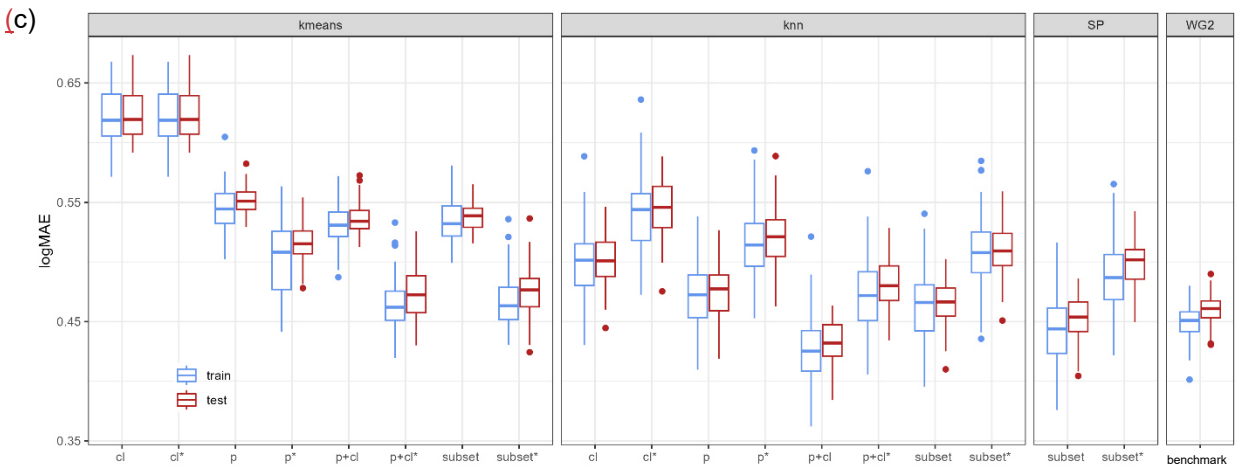
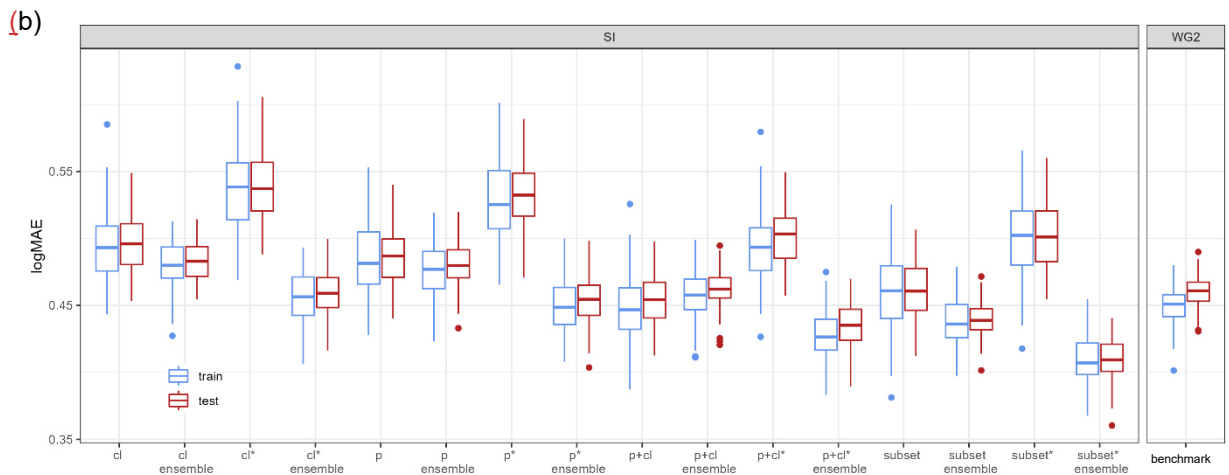
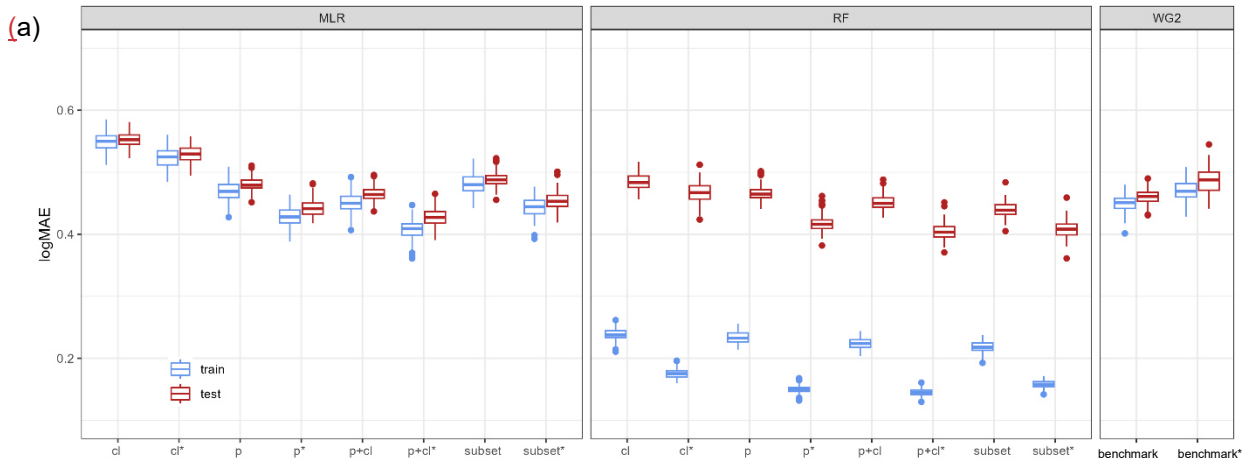
Figure CA2: Distribution of basins descriptors within all basins used for regionalization-regionalization (n=1,236,933)

1013 **Appendix B: Results of split-sample tests**

1014 **Table B1: Summarized results of the split-sample tests for all regionalization methods**

input	method	train (median)	train (sd)	test (median)	test (sd)
-	WG2	1.527	0.042	1.544	0.046
-	SP	-	-	1.356	0.057
el	MLR	1.474	0.039	1.485	0.019
p		1.871	0.034	1.881	0.015
p+el		1.457	0.038	1.473	0.018
all		1.394	0.039	1.425	0.024
el	MLR_t	1.322	0.040	1.331	0.027
p		1.830	0.041	1.843	0.030
p+el		1.307	0.042	1.337	0.030
all		1.245	0.042	1.292	0.034
el	RF	0.688	0.026	1.401	0.029
p		0.741	0.027	1.579	0.032
p+el		0.620	0.020	1.312	0.025
all		0.624	0.021	1.346	0.023
el	RF_t	0.465	0.020	1.310	0.039
p		0.494	0.023	1.540	0.042
p+el		0.378	0.017	1.183	0.037
all		0.345	0.014	1.181	0.034
el	SI_t	1.477	0.080	1.492	0.056
p		1.651	0.086	1.661	0.063
p+el		1.380	0.066	1.375	0.050
all		1.367	0.069	1.390	0.064
el	SI_10	1.398	0.046	1.397	0.029
p		1.558	0.047	1.556	0.027
p+el		1.326	0.044	1.321	0.025
all		1.398	0.049	1.402	0.028
el	SI_10_t	1.281	0.053	1.281	0.043
p		1.497	0.050	1.487	0.037
p+el		1.206	0.048	1.201	0.040
all		1.286	0.053	1.296	0.039
el	k-means	1.689	0.038	1.699	0.018
p		1.910	0.051	1.918	0.039
p+el		1.632	0.046	1.648	0.022
all		1.642	0.044	1.638	0.025
el	k-means_t	1.474	0.111	1.519	0.088
p		1.909	0.055	1.918	0.040
p+el		1.399	0.070	1.425	0.053
all		1.426	0.068	1.417	0.051
el	k-means flexible	1.065	0.048	1.553	0.097
p		1.191	0.046	1.991	0.142
p+el		0.982	0.040	1.568	0.125
all		0.957	0.044	1.515	0.114

1015 **Appendix D: Results of the ensemble of the split-sample tests**



1019 **Figure D1: logMAE values for all 100 split-sampling tests using all variants of a) MLR, RF, and benchmark-to-beat,**
 1020 **b) SI, and c) kmeans, knn, and SP. Note that the asterisk * indicates the tuned version of the method.**

1022
1023

Table D1: Performance loss in median logMAE of the ensemble of split-sample tests from training to testing expressed in % of logMAE in training.

<u>test</u> (% train)	<u>MLR</u>	<u>RF</u>	<u>no ens.</u>	<u>SI</u> <u>ensem-</u> <u>ble</u>	<u>kmeans</u>	<u>knn</u>	<u>SP</u>	<u>B2B</u>
<u>cl</u>	<u>100.4</u>	<u>202.9</u>	<u>100.6</u>	<u>100.6</u>	<u>100</u>	<u>100</u>		
<u>p</u>	<u>102.1</u>	<u>199.6</u>	<u>101.2</u>	<u>100.6</u>	<u>101.3</u>	<u>101.1</u>	<u>102.3</u>	<u>102.2</u>
<u>p+cl</u>	<u>103.1</u>	<u>207.1</u>	<u>101.6</u>	<u>100.9</u>	<u>100.6</u>	<u>95.6</u>		
<u>subset</u>	<u>101.7</u>	<u>223.9</u>	<u>100</u>	<u>100.7</u>	<u>101.3</u>	<u>100.2</u>		

<u>test*</u> (% train*)	<u>MLR</u>	<u>RF</u>	<u>no ens.</u>	<u>SI</u> <u>ensem-</u> <u>ble</u>	<u>kmeans</u>	<u>knn</u>	<u>SP</u>	<u>B2B</u>
<u>cl</u>	<u>100.8</u>	<u>266.9</u>	<u>99.8</u>	<u>100.7</u>	<u>100</u>	<u>100.4</u>		
<u>p</u>	<u>103</u>	<u>277.3</u>	<u>101.3</u>	<u>101.3</u>	<u>101.4</u>	<u>101.4</u>	<u>103.1</u>	<u>104.1</u>
<u>p+cl</u>	<u>104.4</u>	<u>277.9</u>	<u>102</u>	<u>102.1</u>	<u>102.2</u>	<u>101.7</u>		
<u>subset</u>	<u>102</u>	<u>258.2</u>	<u>99.8</u>	<u>100.5</u>	<u>103</u>	<u>100.2</u>		

1024
1025

1026 **References**

- 1027 Arheimer, B., Pimentel, R., Isberg, K., Crochemore, L., Andersson, J. C. M., Hasan, A., & Pineda, L.: Global
1028 catchment modelling using World-Wide HYPE (WWH), open data, and stepwise parameter estimation, *Hydrology
1029 and Earth System Sciences*, 24(2), 535–559. <https://doi.org/10.5194/hess-24-535-2020>, 2020.
- 1030 Arsenault, R., & Brissette, F. P.: Continuous streamflow prediction in ungauged basins: The effects of equifinality
1031 and parameter set selection on uncertainty in regionalization approaches, *Water Resources Research*, 50, 6135–
1032 6153, <https://doi.org/10.1002/2013WR014898>, 2014.
- 1033 Ayzel, G. V., Gusev, E. M., & Nasonova, O. N.: River runoff evaluation for ungauged watersheds by SWAP
1034 model. 2. Application of methods of physiographic similarity and spatial geostatistics, *Water Resources*, 44(4),
1035 547–558, <https://doi.org/10.1134/S0097807817040029>, 2017.
- 1036 Barbarossa, V., Bosmans, J., Wanders, N., King, H., Bierkens, M. F. P., Huijbregts, M. A. J., & Schipper, A. M.:
1037 Threats of global warming to the world's freshwater fishes, *Nature Communications*, 12(1), 1701,
1038 <https://doi.org/10.1038/s41467-021-21655-w>, 2021.
- 1039 Batjes, N. H.: ISRIC-WISE derived soil properties on a 5 by 5 arc-minutes global grid (ver. 1.2) [data set],
1040 <https://data.isric.org/geonetwerk/srv/eng/catalog.search#/metadata/82f3d6b0-a045-4fe2-b960-6d05bc1f37c0>,
1041 2012~~3~~.
- 1042 Beck, H. E., Pan, M., Lin, P., Seibert, J., van Dijk, A. I. J. M., & Wood, E. F.: Global Fully Distributed Parameter
1043 Regionalization Based on Observed Streamflow From 4,229 Headwater Catchments, *Journal of Geophysical Re-
1044 search: Atmospheres*, 125(17), <https://doi.org/10.1029/2019JD031485>, 2020.
- 1045 Beck, H. E., van Dijk, A. I. J. M., Roo, A. de, Dutra, E., Fink, G., Orth, R. & Schellekens, J.: Global evaluation of
1046 runoff from 10 state-of-the-art hydrological models, *Hydrol. Earth Syst. Sci.*, 21, 2881-20903,
1047 <https://doi.org/10.5194/hess-21-2881-2017>, 2017.
- 1048 Beck, H. E., van Dijk, A. I. J. M., Roo, A. de, Miralles, D. G., McVicar, T. R., Schellekens, J., & Bruijnzeel, L.
1049 A.: Global-scale regionalization of hydrologic model parameters, *Water Resources Research*, 52(5), 3599–3622,
1050 <https://doi.org/10.1002/2015WR018247>, 2016.
- 1051 [Benjamini, Y., & Hochberg, Y: Controlling the False Discovery Rate: A Practical and Powerful Approach to](#)
1052 [Multiple Testing, *Journal of the Royal Statistical Society. Series B \(Methodological\)*, 57\(1\), 289–300.](#)
1053 <http://www.jstor.org/stable/2346101>, 1995.
- 1054 Boulange, J, Hanasaki, N, Yamazaki, D., & Pokhrel, Y.: Role of dams in reducing global flood exposure under
1055 climate change, *Nature Communications*, 12(1), 417, <https://doi.org/10.1038/s41467-020-20704-0>, 2021.
- 1056 Breimann, L.: Random Forests, *Machine Learning*, 45, 1–32, <https://doi.org/10.1023/A:1010933404324>, 2001.
- 1057 Chaney, N. W., Herman, J. D., Ek, M. B., & Wood, E. F.: Deriving global parameter estimates for the Noah land
1058 surface model using FLUXNET and machine learning, *Journal of Geophysical Research: Atmospheres*, 121(22),
1059 13,218–13,235, <https://doi.org/10.1002/2016JD024821>, 2016.
- 1060 [Charrad, M., Ghazzali, N., Boiteau, V., Niknafs, A.: NbClust: An R Package for Determining the Relevant Number](#)
1061 [of Clusters in a Data Set, *Journal of Statistical Software*, 61\(6\), 1–36. https://doi.org/10.18637/jss.v061.i06](#), 2014.

1062 Cuntz, M., Mai, J., Samaniego, L., Clark, M., Wulfmeyer, V., Branch, O., Attinger, S., & Thober, S.: The impact
1063 of standard and hard-coded parameters on the hydrologic fluxes in the Noah-MP land surface model, *Journal of*
1064 *Geophysical Research: Atmospheres*, 121, 10,676 - 10,700, <https://doi.org/10.1002/2016JD025097>, 2016.

1065 Döll, P. & Fiedler, K.: Global-scale modeling of groundwater recharge, *Hydrol. Earth Syst. Sci.*, 12, 863–885,
1066 <https://doi.org/10.5194/hess-12-863-2008>, 2008

1067 Döll, P., Kaspar, F., & Lehner, B.: A global hydrological model for deriving water availability indicators: model
1068 tuning and validation, *Journal of Hydrology*, 270, 105–13, [https://doi.org/10.1016/S0022-1694\(02\)00283-4](https://doi.org/10.1016/S0022-1694(02)00283-4), 2003.

1069 [Döll, P., Hasan, H. M. M., Schulze, K., Gerdener, H., Börger, L., Shadkam, S., Ackermann, S., Hosseini-Moghari,](#)
1070 [S.-M., Müller Schmied, H., Güntner, A., & Kusche, J.: everaging multi-variable observations to reduce and quan-](#)
1071 [tify the output uncertainty of a global hydrological model: evaluation of three ensemble-based approaches for the](#)
1072 [Mississippi River basin, *Hydrology and Earth System Sciences*, 28 \(10\), 2259-2295, \[https://doi.org/10.5194/hess-\]\(https://doi.org/10.5194/hess-28-2259-2024\)](#)
1073 [28-2259-2024, 2024.](#)

1074 [Draper, C. S., Walker, J. P., Steinle, P. J., de Jeu, R. A. M., Holmes T. R. H.: An evaluation of AMSR–E derived](#)
1075 [soil moisture over Australia, *Remote Sensing of Environment*, 113, 703-710,](#)
1076 [<https://doi.org/10.1016/j.rse.2008.11.011>, 2008.](#)

1077 Eisner, S.: Comprehensive Evaluation of the WaterGAP3 Model across Climatic, Physiographic, and Anthropo-
1078 genic Gradients, Ph.D. thesis, University of Kassel, Kassel, Germany, 128pp., 2016.

1079 Friedl, M., Sulla-Menashe, D.: MCD12Q1 MODIS/Terra+Aqua Land, Cover Type Yearly L3 Global 500m SIN
1080 Grid V006, [NASA EOSDIS Land Processes DAAC](#) [data set], ~~[NASA EOSDIS Land Processes DAAC](#)~~,
1081 <https://doi.org/10.5067/MODIS/MCD12Q1.006>, 2019.

1082 Feigl, M., Thober, S., Schweppe, R., Herrnegger, M., Samaniego, L., & Schulz, K.: Automatic Regionalization of
1083 Model Parameters for Hydrological Models, *Water Resources Research*, 58, e2022WR031966,
1084 <https://doi.org/10.1029/2022WR031966>, 2022.

1085 Golian, S., Murphy, C., & Meresa, H.: Regionalization of hydrological models for flow estimation in ungauged
1086 catchments in Ireland, *Journal of Hydrology: Regional Studies*, 36, 100859,
1087 <https://doi.org/10.1016/j.ejrh.2021.100859>, 2021.

1088 GRDC, The Global Runoff Data Centre, 56068 Koblenz, Germany, 2020.

1089 [Gudmundsson, L., Tallaksen, L. M., Stahl, K., Clark, D. B., Dumont, E., Hagemann, S., Bertrand, N., Gerten, D.,](#)
1090 [Heinke, J., Hanasaki, N., Voss, F., & Koirala, S.: Comparing Large-Scale Hydrological Model Simulations to](#)
1091 [Observed Runoff Percentiles in Europe. *Journal of Hydrometeorology*, 13\(2\), 604-620.](#)
1092 [<https://doi.org/10.1175/JHM-D-11-083.1>, 2012.](#)

1093

1094 Guo Y, Zhang Y, Zhang L, & Wang Z: Regionalization of hydrological modeling for predicting streamflow in
1095 ungauged catchments: A comprehensive review, *WIREs Water*, 8, e1487, <https://doi.org/10.1002/wat2.1487>,
1096 2020.+

1097 Gupta, H. V, Sorooshian, S., & Yapo, P. O.: Toward improved calibration of hydrologic models: Multiple and
1098 noncommensurable measures of information, *Water Resources Research*, 34(4), 751–763,
1099 <https://doi.org/10.1029/97WR03495>, 1998.

1100 He, Y., Bárdossy, A., & Zehe, E.: A review of regionalisation for continuous streamflow simulation, *Hydrology
1101 and Earth System Sciences*, 15(11), 3539–3553. <https://doi.org/10.5194/hess-15-3539-2011>, 2011.

1102 [Jansen, K. F., Teuling, A. J., Craig, J. R., Dal Molin, M., Knoben, W. J. M., Parajka, J., Vis, M., Melsen, L. A.:](#)
1103 [Mimicry of a conceptual hydrological model \(HBV\): What's in a name? *Water Resources Research*, 57,](#)
1104 [e2020WR029143. <https://doi.org/10.1029/2020WR029143>, 2022.](#)

1105 Kaspar, F.: Entwicklung und Unsicherheitsanalyse eines globalen hydrologischen Modells, Ph.D. thesis, Univer-
1106 sity of Kassel, Kassel, Germany, 129pp., 2004.

1107 [Khosa, F. V., Mateyisi, M. J., van der Merwe, M. R., Feig, G. T., Engelbrecht, F. A., Savage, M. J.: Evaluation of](#)
1108 [soil moisture from CCAM-CABLE simulation, satellite-based models estimates and satellite observations: a case](#)
1109 [study of Skukuza and Malopeni flux towers, *Hydrology and Earth System Sciences*, 24\(4\), 1587-1609,](#)
1110 [https://doi.org/10.5194/hess-24-1587-2020, 2020.](#)

1111 Krabbenhoft, C. A., Allen, G. H., Lin, P., Godsey, S. E., Allen, D. C., Burrows, R. M., DelVecchia, A. G., Fritz,
1112 K. M., Shanafield, M., Burgin, A. J., Zimmer, M. A., Detry, T., Dodds, W. K., Jones, C. N., Mims, M. C., Franklin,
1113 C., Hammond, J. C., Zipper, S., Ward, A. S., Olden, J. D.: Assessing placement bias of the global river gauge
1114 network, *Nature Sustainability*, 5, 586–592. <https://doi.org/10.1038/s41893-022-00873-0>, 2022.

1115 Kupzig, J., Reinecke, R., Pianosi, F., Flörke, M., & Wagener, T.: Towards parameter estimation in global hydro-
1116 logical models, *Environmental Research Letters*, 18(7), 74023. <https://doi.org/10.1088/1748-9326/acdae8>, 2023.

1117 Lange, S.: Earth2Observe, WFDEI and ERA-Interim data Merged and Bias-corrected for ISIMIP (EWEMBI), V.
1118 1.1, [GFZ Data Services](#) [data set]; ~~GFZ Data Services~~, <https://doi.org/10.5880/pik.2019.004>, 2019.

1119 Lebecherel, L., Andréassian, V., Perrin: On evaluating the robustness of spatial-proximity-based regionalization
1120 methods, *Journal of Hydrology*, 539, 196-203, <https://doi.org/10.1016/j.jhydrol.2016.05.031>, 2016.

1121 Lehner, B. and Döll, P.: Development and validation of a global database of lakes, reservoirs and wetlands, *Journal
1122 of Hydrology*, 296 (1-4), 1-22, <https://doi.org/10.1016/j.jhydrol.2004.03.028>, 2004.

1123 Lehner, B., Verdin, K., & Jarvis, A.: New global hydrography derived from spaceborne elevation data, *Eos, Trans-
1124 actions, AGU*, 89, 93–94, doi:10.1029/2008EO100001, 2008.

1125 Liam, A., & Wiener, M.: Classification and Regression by randomForest. *R News*, 2(3), 18–22, 2002.

1126 Lindström, G., Johansson, B., Persson, M., Gardelin, M., & Bergström, S.: Development and test of the distributed
1127 HBV-96 hydrological model, *Journal of Hydrology*, 201, 272–288, [https://doi.org/10.1016/S0022-
1694\(97\)00041-3](https://doi.org/10.1016/S0022-
1128 1694(97)00041-3), 1997.

1129 McIntyre, N, Lee, H., Wheeler, H., Young, A., & Wagener, T.: Ensemble predictions of runoff in ungauged catch-
1130 ments, *Water Resources Research*, 41(12), W12434, <https://doi.org/10.1029/2005WR004289>, 2005.

1131 [Merz, R., Blöschl, G.: Regionalisation of catchment model parameters, *Journal of Hydrology*, 287, 95-123,](#)
1132 [https://doi.org/10.1016/j.jhydrol.2003.09.028, 2004.](#)

1133 Müller Schmied, H., Cáceres, D., Eisner, S., Flörke, M., Herbert, C., Niemann, C., Peiris, T. A., Popat, E., Port-
1134 mann, F. T., Reinecke, R., Schumacher, M., Shadkam, S., Telteu, C.-E., Trautmann, T., -Döll, P.: The global water
1135 resources and use model WaterGAP v2.2d: model description and evaluation, *Geoscientific Model Development*,
1136 14(2), 1037–1079, <https://doi.org/10.5194/gmd-14-1037-2021>, 2021.

1137 [Müller Schmied, H., Trautmann, T., Ackermann, S., Cáceres, D., Flörke, M., Gerdener, H., Kynast, E., Peiris, T.](#)
1138 [A., Schiebener, L., Schumacher, M., Döll, P.: The global water resources and use model WaterGAP v2.2e: de-](#)
1139 [scription and evaluation of modifications and new features, *Geoscientific Model Development Discussions* \[pre-](#)
1140 [print\], 1-46, <https://doi.org/10.5194/gmd-2023-213>, 2023.](#)

1141 Nijssen, B., O'Donnell, G. M., Lettenmeier, D. P., Lohmann, D., & Wood, E. F.: Predicting the Discharge of
1142 Global Rivers, *American Meteorological Society*, 3307–3323, [https://doi.org/10.1175/1520-](https://doi.org/10.1175/1520-0442(2001)014<3307:PTDOGR>2.0.CO;2)
1143 [0442\(2001\)014<3307:PTDOGR>2.0.CO;2](https://doi.org/10.1175/1520-0442(2001)014<3307:PTDOGR>2.0.CO;2), 2000.

1144 [Oloruntoba, B., Kollet, S., Motzka, C., Vereecken H., Franssen H.-J. H.: High Resolution Land Surface Modelling](#)
1145 [over Africa: the role of uncertain soil properties in combination with temporal model resolution, *EGUsphere Pre-*](#)
1146 [print repository \[preprint\], <https://doi.org/10.5194/egusphere-2023-3132>, 2024.](#)

1147 Oudin, L., Andréassian, V., Perrin, C., Michel, C., & Le Moine, N.: Spatial proximity, physical similarity, regres-
1148 sion and ungauged catchments: A comparison of regionalization approaches based on 913 French catchments, *Water*
1149 *Resources Research*, 44(3), W03413, <https://doi.org/10.1029/2007WR006240>, 2008.

1150 Oudin, L., Kay, A., Andréassian, V., & Perrin, C.: Are seemingly physically similar catchments truly hydrologi-
1151 cally similar? *Water Resources Research*, 46(11), W11558, <https://doi.org/10.1029/2009WR008887>, 2010.

1152 Pagliero, L., Bouraoui, F., Diels, J., Willems, P., & McIntyre, N.: Investigating regionalization techniques for
1153 large-scale hydrological modelling, *Journal of Hydrology*, 570, 220–235, [https://doi.org/10.1016/j.jhyd-](https://doi.org/10.1016/j.jhydrol.2018.12.071)
1154 [rol.2018.12.071](https://doi.org/10.1016/j.jhydrol.2018.12.071), 2019.

1155 Parajka, J., Merz, R., & Blöschl, G.: A comparison of regionalisation methods for catchment model parameters,
1156 *Hydrology and Earth System Sciences*, 9, 157–171, <https://doi.org/10.5194/hess-9-157-2005>, 2005.

1157 ~~[Parajka, J., Viglione, A., Rogger, M., Salinas, J. L., Sivaplan, M. & Blöschl, G.: Comparative assessment of pre-](#)~~
1158 ~~[diction in ungauged basins—Part 1: Runoff hydrograph studies, *Hydrology and Earth System Sciences*, 17, 1783-](#)~~
1159 ~~[1795, \[www.hydrol-earth-syst-sci.net/17/1783/2013/\]\(http://www.hydrol-earth-syst-sci.net/17/1783/2013/\), 2013.](#)~~

1160 Poissant, D., Arsenault, R. & Brissette, F.: Impact of parameter set dimensionality and calibration procedures on
1161 streamflow prediction at ungauged catchments, *Journal of Hydrology: Regional Studies*, 12, 220–237,
1162 <https://doi.org/10.1016/j.ejrh.2017.05.005>, 2017.

1163 Pool, S., Vis, M., & Seibert, J.: Regionalization for ungauged catchments — Lessons learned from a comparative
1164 large-sample study. *Water Resources Research*, 57, e2021WR030437. <https://doi.org/10.1029/2021WR030437>,
1165 2021.

1166 Qi, W., Chen, J., Li, L., Xu, C., Li, J., Xiang, Y., & Zhang, S.: A framework to regionalize conceptual model
1167 parameters for global hydrological modelling, *Hydrology and Earth System Sciences Discussions* [preprint],
1168 <https://doi.org/10.5194/hess-2020-127>, 2020.

1169 R Core Team.: R: A language and environment for statistical computing R Foundation for Statistical Computing,
1170 Vienna, Austria. <https://www.r-project.org/>, 2020.

1171 Reichl, J. P. C., Western, A. W., McIntyre, N. R. & Chiew, F. H. S.: Optimization of a Similarity Measure for
1172 Estimating Ungauged Streamflow, *Water Resources Research*, 45 (10), <https://doi.org/10.1029/2008WR007248>,
1173 2009

1174 Samaniego, L, Kumar, R & Attinger, S.: Multiscale parameter regionalization of a grid-based hydrologic model
1175 at the mesoscale, *Water Resources Research*, 46(5), W05523, <https://doi.org/10.1029/2008WR007327>, 2010.

1176 Schaeffli, B., & Gupta, H. V.: Do Nash values have value?, *Hydrological Processes*, 21(15), 2075–2080,
1177 <https://doi.org/10.1002/hyp.6825>, 2007.

1178 Schweppe, R., Thober, S., Müller, S., Kelbling, M., Kumar, R., Attinger, S., & Samaniego, L.: MPR 1.0: a stand-
1179 alone multiscale parameter regionalization tool for improved parameter estimation of land surface models, *Geo-
1180 scientific Model Development*, 15, 859–882, <https://doi.org/10.5194/gmd-15-859-2022>, 2022.

1181 Seibert, J.: On the need for benchmarks in hydrological modelling, *Hydrological Processes*, 15(6), 1063–1064,
1182 <https://doi.org/10.1002/hyp.446>, 2001.

1183 Shannon, C. E.: A Mathematical Theory of Communication, *The Bell System Technical Journal*, 3(27), 379-423,
1184 <https://doi.org/10.1002/j.1538-7305.1948.tb01338.x>, 1948.

1185 Stacke, T., & Hagemann, S.: HydroPy (v1.0): a new global hydrological model written in Python, *Geoscientific
1186 Model Development*, 14, 7795–7816, <https://doi.org/10.5194/gmd-14-7795-2021>, 2021.

1187 Tang, Y., Marshall, L., Sharma, A. & Smith, T.: Tools for investigating the prior distribution in Bayesian hydrology,
1188 *Journal of Hydrology*, 538, 551-562, <https://doi.org/10.1016/j.jhydrol.2016.04.032>, 2016.

1189 Tongal, H., & Sivakumar, B.: Cross-entropy clustering framework for catchment classification, *Journal of Hydrology*,
1190 552, 433–446, <https://doi.org/10.1016/j.jhydrol.2017.07.005>, 2017.

1191 Venables, W. N., & Ripley, B. D.: *Modern Applied Statistics with S (Fourth Edition)*. Springer Science+Business
1192 Media New York, USA, 501pp, ISBN 978-1-4419-3008-8, 2002

1193 Wagener, T., Wheater, H. S., & Gupta, H. V. ~~(2004)~~: *Rainfall – Runoff Modelling in Gauged and Ungauged
1194 Catchments*, Imperial College Press, London, UK, 332pp., <https://doi.org/10.1142/p335>, 2004.

1195 [Wagener, T., & Wheater, H. S.: Parameter estimation and regionalization for continuous rainfall-runoff models
1196 including uncertainty, *Journal of Hydrology*, 320, 132-154, <https://doi.org/10.1016/j.jhydrol.2005.07.015>, 2006.](#)

1197 [Ward, P. J., Jongman, B., Sperna Weiland, F., Bouwman, A., Van Beek, R., Bierkens, M. F. P., Ligtoet, W., &
1198 Winsemius, H. C.: Assessing flood risk at the global scale: model setup, results, and sensitivity, *Environmental
1199 Research Letters*, 8, Article 044019. <https://doi.org/10.1088/1748-9326/8/4/044019>, 2013](#)

1200 Widén-Nilsson, E., Halldin, S., & Xu, C.: Global water-balance modelling with WASMOD-M: Parameter estimation
1201 and regionalisation, *Journal of Hydrology*, 340(1-2), 105–118, <https://doi.org/10.1016/j.jhydrol.2007.04.002>,
1202 2007.

- 1203 Wu, H., Zhang, J., Bao, Z., Wang, G., Wang, W., Yang, Y. & Wang, J.: Runoff Modeling in Ungauged Catchments
1204 Using Machine Learning Algorithm-Based Model Parameters Regionalization Methodology, *Engineering*, 28, 93-
1205 104, <https://doi.org/10.1016/j.eng.2021.12.014>, 2023.
- 1206 Yang, X., Magnusson, J., Huang, S., Beldring, S., & Xu, C.: Dependence of regionalization methods on the com-
1207 plexity of hydrological models in multiple climatic regions, *Journal of Hydrology*, 582, 124357,
1208 <https://doi.org/10.1016/j.jhydrol.2019.124357>, 2020.
- 1209 Yoshida, T., Hanasaki, N, Nishina, K., Boulange, J, Okada, M., & Troch, P. A.: Inference of Parameters for a
1210 Global Hydrological Model: Identifiability and Predictive Uncertainties of Climate-Based Parameters, *Water Re-
1211 sources Research*, 58, e2021WR03066, <https://doi.org/10.1029/2021WR030660>, 2022.